

EUR 4475 e

COMMISSION OF THE EUROPEAN COMMUNITIES

OPEN-VESSEL EXPERIMENTS ON PLUTONIUM PROTOTYPE ELEMENTS IN THE GARIGLIANO REACTOR

by

A. ARIEMMA*, L. BRAMATI*, U. CAMMAROTA*, M. GALLIANI*,
A. GIBELLO**, G. LESNONI*, M. MIRONE*, M. PAOLETTI-GUALANDI*,
P. PERONI*, H. VANDENBROECK*** and B. ZAFFIRO*

* ENEL, Rome (Italy)

** CNEN, Rome (Italy)

*** CEN/SCK, Mol (Belgium)

1970



Report prepared by ENEL
Ente Nazionale per l'Energia Elettrica
Direzione delle Costruzioni Termiche e Nucleari
Rome - Italy

Euratom Contract No. 092-66-6 TEEI

LEGAL NOTICE

This document was prepared under the sponsorship of the Commission of the European Communities.

Neither the Commission of the European Communities, its contractors nor any person acting on their behalf :

make any warranty or representation, express or implied, with respect to the accuracy, completeness, or usefulness of the information contained in this document, or that the use of any information, apparatus, method, or process disclosed in this document may not infringe privately owned rights; or

assume any liability with respect to the use of, or for damages resulting from the use of any information, apparatus, method or process disclosed in this document.

This report is on sale at the addresses listed on cover page 4

at the price of FF 11.—	FB 100.—	DM 7.30	Lit. 1,250	Fl. 7.25
-------------------------	----------	---------	------------	----------

When ordering, please quote the EUR number and the title, which are indicated on the cover of each report.

Printed by ENEL - Rome
Luxembourg, April 1970

EUR 4475 e

OPEN-VESSEL EXPERIMENTS ON PLUTONIUM PROTOTYPE ELEMENTS IN THE GARIGLIANO REACTOR,
by A. ARIEMMA*, L. BRAMATI*, U. CAMMAROTA*, M. GALLIANI*,
A. GIBELLO**, G. LESNONI*, M. MIRONE*, M. PAOLETTI-GUALANDI*,
P. PERONI*, H. VANDENBROECK*** and B. ZAFFIRO*

* ENEL, Rome (Italy), ** CNEN, Rome (Italy), *** CEN/SCK, Mol (Belgium)

Commission of the European Communities

Report prepared by ENEL - Ente Nazionale per l'Energia Elettrica

Direzione delle Costruzioni Termiche e Nucleari - Rome (Italy)

Euratom Contract No. 092-66-6 TEE1

Luxembourg, April 1970 - 68 Pages - 25 Figures - BF 100

During the last shutdown of the Garigliano reactor for refuelling (August-September 1968), a series of critical experiments were performed on assemblies containing reload enriched-uranium elements and prototype plutonium elements. The outcome of these experiments was information on the rod power density distributions associated with highly heterogeneous lattices and reactivity

EUR 4475 e

OPEN-VESSEL EXPERIMENTS ON PLUTONIUM PROTOTYPE ELEMENTS IN THE GARIGLIANO REACTOR,
by A. ARIEMMA*, L. BRAMATI*, U. CAMMAROTA*, M. GALLIANI*,
A. GIBELLO**, G. LESNONI*, M. MIRONE*, M. PAOLETTI-GUALANDI*,
P. PERONI*, H. VANDENBROECK*** and B. ZAFFIRO*

* ENEL, Rome (Italy), ** CNEN, Rome (Italy), *** CEN/SCK, Mol (Belgium)

Commission of the European Communities

Report prepared by ENEL - Ente Nazionale per l'Energia Elettrica

Direzione delle Costruzioni Termiche e Nucleari - Rome (Italy)

Euratom Contract No. 092-66-6 TEE1

Luxembourg, April 1970 - 68 Pages - 25 Figures - BF 100

During the last shutdown of the Garigliano reactor for refuelling (August-September 1968), a series of critical experiments were performed on assemblies containing reload enriched-uranium elements and prototype plutonium elements. The outcome of these experiments was information on the rod power density distributions associated with highly heterogeneous lattices and reactivity

variations following replacement of enriched-uranium elements with plutonium elements.

The technique used for power density measurements (gamma activity scanning by means of a NaI crystal) proved its outstanding capabilities, because it revealed minor effects on the power densities, such as those due to rod manufacturing tolerances.

The good agreement observed in previous criticality experiments between the experimental values and those obtained with the calculation methods adopted by ENEL in the design of plutonium prototype fuel elements was fully confirmed. The power density was calculated with a standard deviation less than 2 %, and reactivity with an error below 0.5 %.

variations following replacement of enriched-uranium elements with plutonium elements.

The technique used for power density measurements (gamma activity scanning by means of a NaI crystal) proved its outstanding capabilities, because it revealed minor effects on the power densities, such as those due to rod manufacturing tolerances.

The good agreement observed in previous criticality experiments between the experimental values and those obtained with the calculation methods adopted by ENEL in the design of plutonium prototype fuel elements was fully confirmed. The power density was calculated with a standard deviation less than 2 %, and reactivity with an error below 0.5 %.

EUR 4475 e

COMMISSION OF THE EUROPEAN COMMUNITIES

OPEN-VESSEL EXPERIMENTS ON PLUTONIUM PROTOTYPE ELEMENTS IN THE GARIGLIANO REACTOR

by

A. ARIEMMA*, L. BRAMATI*, U. CAMMAROTA*, M. GALLIANI*,
A. GIBELLO**, G. LESNONI*, M. MIRONE*, M. PAOLETTI-GUALANDI*,
P. PERONI*, H. VANDENBROECK*** and B. ZAFFIRO*

* ENEL, Rome (Italy)

** CNEN, Rome (Italy)

*** CEN/SCK, Mol (Belgium)

1970



Report prepared by ENEL
Ente Nazionale per l'Energia Elettrica
Direzione delle Costruzioni Termiche e Nucleari
Rome - Italy

Euratom Contract No. 092-66-6 TEEI

ABSTRACT

During the last shutdown of the Garigliano reactor for refuelling (August-September 1968), a series of critical experiments were performed on assemblies containing reload enriched-uranium elements and prototype plutonium elements. The outcome of these experiments was information on the rod power density distributions associated with highly heterogeneous lattices and reactivity variations following replacement of enriched-uranium elements with plutonium elements.

The technique used for power density measurements (gamma activity scanning by means of a NaI crystal) proved its outstanding capabilities, because it revealed minor effects on the power densities, such as those due to rod manufacturing tolerances.

The good agreement observed in previous criticality experiments between the experimental values and those obtained with the calculation methods adopted by ENEL in the design of plutonium prototype fuel elements was fully confirmed. The power density was calculated with a standard deviation less than 2 %, and reactivity with an error below 0.5 %.

KEYWORDS

SHUTDOWN
SENN 1
URANIUM
PLUTONIUM

ELEMENTS
LATTICES
REACTIVITY
NON-DESTRUCTIVE TESTING

INDEX

	Page
1. INTRODUCTION	1
2. FUEL ELEMENTS	1
3. CRITERIA FOLLOWED IN THE PERFORMANCE OF THE CRITICALITY EXPERIMENTS	2
4. CRITICAL CONFIGURATIONS	3
5. POWER DISTRIBUTION MEASUREMENTS	4
5.1 Measurement technique	4
5.2 Fuel rod irradiation and handling	5
5.3 Measurement equipment	7
5.4 Details of the measurements	7
6. ANALYSIS OF EXPERIMENTAL RESULTS	9
6.1 Criticality experiments	9
6.2 Power distributions	11
6.2.1 Level not affected by the control rods	11
6.2.2 Level influenced by the control rods	12
6.2.3 Fine-structure effects	14
7. COMPARISON BETWEEN THE EXPERIMENTAL DATA AND THE CALCULATED VALUES	14
7.1 Theoretical models	14
7.2 Consistency of the experimental and theoretical data	17
7.2.1 Criticality evaluations	17
7.2.2 Power distributions	18
8. CONCLUSIONS	20

BIBLIOGRAPHY

APPENDIX I - Preliminary measurements to set down the technique
for the gamma scanning of Pu fuel rods

APPENDIX II - Description of the measurement and control procedures

- APPENDIX III - La-140 activity-power conversion factors
- APPENDIX IV - Reduction of the total gamma activity data to power density
- APPENDIX V - Criticality tests in the reactor vessel

SUMMARY

During the last shutdown of the Garigliano reactor for refueling (August-September 1968), a series of critical experiments were performed on assemblies containing reload enriched-uranium elements and prototype plutonium elements. The outcome of these experiments was information on the rod power density distributions associated with highly heterogeneous lattices and reactivity variations following replacement of enriched-uranium elements with plutonium elements.

The technique used for power density measurements (gamma activity scanning by means of a NaI crystal) proved its outstanding capabilities, because it revealed minor effects on the power densities, such as those due to rod manufacturing tolerances.

The good agreement observed in previous criticality experiments between the experimental values and those obtained with the calculation methods adopted by ENEL in the design of plutonium prototype fuel elements was fully confirmed. The power density was calculated with a standard deviation less than 2%, and reactivity with an error below 0.5%.

1. Introduction

The experimental and theoretical work described in this report was carried out by ENEL under the Joint ENEL-EURATOM Research Program for plutonium utilization in thermal reactors. During the last shutdown of the Garigliano reactor for refueling (August-September 1968), a series of critical experiments were performed on assemblies containing reload enriched-uranium elements and prototype plutonium elements. The purpose of these experiments was to check the expected performance of plutonium fuel elements by assessing the accuracy of the calculation methods used in the nuclear design of plutonium fuel elements. Since these experiments were performed on full-scale elements, they provide an integration of the experimental data previously obtained by others on critical facilities, such as those at WREC and at PNWL, and by UKAEA at Winfrith on ENEL's behalf⁽¹⁾. In particular, they allow an assessment of the accuracy of the calculations for the determination of K_{∞} and power distribution in mixed lattices, also in relation to the effects of water gaps and proximity of enriched-uranium elements to plutonium elements.

The experiments can be subdivided into two groups:

- a) Criticality experiments
- b) Measurement of the local power distribution through gamma scanning on slightly irradiated fuel rods removed from the assemblies.

2. Fuel elements

Three types of fuel elements were used in these experiments:

- a) normal reload fuel elements enriched on an average to 2.3% U-235 (Fig. 1);
- b) standard plutonium prototype elements (Fig. 2);
- c) mixed uranium-plutonium prototype elements, consisting of 40 enriched uranium rods and 24 plutonium rods (Fig. 3).

The isotopic composition of the plutonium was 88.96% Pu-239, 9.77% Pu-240, 1.19% Pu-241 and 0.08% Pu-242.

The mechanical design was the same for all the elements. Each fuel element contained a square array of 64 fuel rods housed in a square Zircaloy flow channel of 0.20 cm thickness. The pitch of the fuel elements was 17.89 cm, whilst that of the fuel rods within each element was 1.97 cm. The Zircaloy-clad fuel rods were 1.51 cm in diameter, and the pellet was 1.29 cm. The active fuel length was 271.80 cm.

The fuel rods were located and supported at their ends by stainless steel tie plates and held in position along their length by stainless steel spacers (total equivalent weight of SS spacers, 1500 gr). Eight of the peripheral fuel rods (tie rods) had threaded end plugs and were secured to the tie plates to form a box-like structure.

The fundamental criterion followed in the nuclear design of the plutonium elements was that their reactivity life and maximum rod power density were to be the same as those of the reload enriched uranium elements. With regard to the critical experiments, however, it should be noted that, because of the different conversion ratio and of the different hot-to-cold swing, the initial K_{∞} of the standard plutonium elements and mixed uranium-plutonium elements in cold condition is by a few percent greater than the K_{∞} of the enriched-uranium elements.

3. Criteria followed in the performance of the criticality experiments

The purpose of these experiments was to assess the accuracy with which the calculation method determines the K_{∞} of the plutonium elements. In order to obtain meaningful information, it was considered appropriate first to form a critical assembly with all enriched-uranium elements and then to replace these elements one at a time with a plutonium element. Neutron leakage in the radial direction is very high in these critical assemblies and any errors in its evaluation may compensate the errors in the determination of K_{∞} . The criterion of retaining the same geometry in all the critical assemblies would permit any error in the evaluation of neutron leakage to be approximately the same for all the critical assemblies.

The reactor control system (control rods) was not the best suited for the intended purpose; it was therefore necessary to limit the number of replacement plutonium elements in order to assess the reactivity variations with the technique of rising and falling period, thus avoiding the need for a complete calibration of the control rods which is never quite feasible.

4. Critical configurations

The critical assemblies were formed in the reactor pressure vessel. For this purpose the elements of a whole core quadrant were discharged to leave room for the critical assemblies. The latter were separated from the irradiated elements by a water belt at least 60 cm wide, which was enough to exclude any chance of neutron interaction and to lower the gamma background to acceptable limits (Fig. 4).

As expected on the basis of the theoretical evaluation, seven enriched-uranium elements were required to attain criticality. The first criticality was obtained with seven control rods (E9, E10, F8, F9, F10, G9, G10) banked to notch in the midst of or adjacent to fuel elements.^(*)

Period measurements, carried out about 30 hours after first criticality, showed no reactivity variation in time. It was found that when the two control rods, F9 and F10, surrounded by the fuel, were inserted one more notch, the five control rods around the edge of the load could be fully withdrawn. Control rods F9 and F10 were then calibrated around notch 18 by the technique of successive rising and falling periods.

The various configurations obtained with the successive replacements were:(Fig. 5):

- Configuration II : A standard plutonium element loaded into a corner position
- Configuration III : The standard plutonium element shifted to the opposite corner position
- Configuration IV : The standard plutonium element loaded into a more central position

(*) A detailed description of the procedures and of the problems encountered is given in Appendix V.

4.

- Configuration V: A mixed uranium-plutonium element substituted for the plutonium element in the preceding configuration.

Calibration of rods F9 and F10 was repeated for the various configurations. Thus, it was possible to make several configurations with the control rods at the same levels, so that the ΔK involved in a replacement could be assessed on the basis of the difference between the related periods.

Configuration III, which is practically equal to Configuration II, was formed to check the reproducibility of a critical configuration. The only difference was that in Configuration II control rod F9 was adjacent to a plutonium element, whereas in Configuration III it was completely surrounded by uranium elements.

The water temperature at the inlet and outlet of the unloading system remained practically constant at 23°C throughout the tests. Chemical analyses of the water did not reveal the presence of any poison in the moderator.

5. Power distribution measurements

5.1 Measurement technique

The power distribution measurements consisted in slightly irradiating the fuel elements of a critical assembly and in monitoring the 1.6-MeV gamma activity of the Ba-140/La-140 chain on the individual rods.

The La-140 gamma scan was preferred to the measurement of the total fission product gamma activity because the decay law of the Ba-La chain is obviously independent of the fissile material composition, and the correlation factor between gamma activity and power can be calculated with fair approximation for various types of rods. This is not so for the total gamma activity.

Indeed, a few preliminary measurements of the total activity, performed previous to the formation of the critical assemblies (Appendix I), had indicated a substantial difference between the decay laws of the various

types of rods. The acceptance of these laws would have entailed a periodical scan of all the typical rods (seven) which it was instead desirable to avoid in order to safeguard rod integrity and minimize measurement times. In addition, it was practically impossible to obtain the gamma activity/power correlation factors for the various types of rods with sufficient precision other than by supplementing the total gamma activity values with those of the La-140 activity.

5.2 Fuel rod irradiation and handling

Symmetry requirements led to the choice of an assembly of nine fuel elements in a 3x3 array. Four were enriched-uranium elements, four were mixed plutonium-uranium elements and the one in the center was a standard plutonium element in order to provide a wider range of information.

The reactivity of this critical assembly was estimated previously by means of a 5-group bidimensional diffusion calculation. On the basis of the information obtained through this calculation, the four uranium elements and the central plutonium element were housed in stainless steel rather than Zircaloy flow channels, to limit the excess reactivity of the assembly and thus the degree of control rod insertion. The use of the stainless steel flow channels lowered the K_{eff} to 1.006.

Under these conditions it should have been possible to obtain a sufficiently flat radial power distribution at a level of interest without any disturbance from the control rod bank. The configuration thus selected (Fig. 6) was characterized by a high degree of symmetry and by the presence of all three types of elements in one octant. This permitted the gamma scanning to be concentrated on the rods of an octant.

With the control rod bank nearly all out (70 cm insertion, corresponding to $\Delta K = 0.006$), the 3x3 configuration reached criticality, thus confirming the theoretical prediction.

The nine-element assembly was irradiated at a neutron flux of about 10^9 nv for about an hour.

The irradiation conditions had been established previously on the basis of preliminary measurements taken on specimens of three types of the rods contained in the fuel elements (see Appendix I). These conditions represent a satisfactory compromise between the requirement of sufficient La-140 gamma activity for the measurement, and the necessity of keeping the radiation level low enough to permit rod handling without undue exposure of the personnel. A second set of specimens was placed inside an aluminium dummy element located at the boundary of the 3x3 configuration (Fig. 6). This second set was used to check the gamma activity decay laws, because the impracticability of handling the rods did not permit them to be subjected to periodical measurements.

Three fuel elements, that is, one reload fuel element, one standard plutonium and one mixed uranium-plutonium fuel element present in the same octant, were all transferred to the pool and allowed to decay for fourteen days. This waiting period was necessary to obtain meaningful data from the La-140 gamma scan. Indeed, after about two weeks from irradiation, the 1.6-MeV gamma activity of La-140 is still high, and the interference of the other fission products is negligible.

After this hold-up period, the elements were decontaminated and transferred one at a time to the fresh fuel vault where they were disassembled and gamma-scanned. In this manner, handling of the plutonium rods occurred in a restricted area and could easily be kept under control.

Before starting the disassembly operations, the element was monitored to ascertain that the dose was lower than the specified limit. The station equipment normally used for fuel element inspection was employed for the disassembly (Fig. 7). The personnel assigned to this operation had been trained on a full-scale fuel element mock-up, specially procured for this purpose.

Disassembly consisted in removing the upper tie plate from the eight tie rods (Fig. 8). Since the other rods of the fuel element simply rested on the lower plate, they could be raised manually with the aid of a constant-load hoist. Once removed from the fuel element, each rod was placed in an aluminium protection tube (Fig. 9) where it remained throughout the transfer and counting operations up to the time it was to be placed back into the fuel element.

Not more than two rods were removed at a time to avoid the risk of altering the fuel element arrangement and jeopardizing its rigidity.

5.3 Measurement equipment

The equipment used for gamma scanning comprised:

- An auxiliary system for positioning and rotation of the rods (Fig. 10).
- A shielding and collimation system made of lead bricks.
- Two counting chains, each consisting of a photoscintillator (NaI), a multi-channel (400 channels) pulse analyzer and a fast printer (Figs 11 and 12).

The rod positioning and rotating system comprised a jib crane for the vertical movement of the protection tube, a hooking and ball bearing rotating system, a fixed system to guide the aluminium tube in front of the slit in the shield, and a locking and rotating system.

The shielding and monitoring system consisted of a parallelepiped lead-brick shield enclosing two photoscintillators with a 2" x 2" NaI crystal and the related preamplifiers. The two detectors were located in front of the collimator at an angle of 30° and at a distance of about 15 cm from the rod. The collimator was 3 cm wide. The entire system weighed three tons and was supported by a steel base about 3 m high.

The size of the collimator slit was chosen rather large to minimize the influence of pellet dishing.

The pulse analysing system comprised two 400-channel spectrum analyzers of LABEN make, complete with HV power supplies, amplifier, timer, integrator between two preset channels, multiscaler and printer of the memory content.

5.4 Details of the measurements (*)

With the equipment described above it was possible to duplicate the measurements and at the same time to determine the 1.6-MeV gamma activity of La-140 by integrating the pulses over the whole area of the 1.6-MeV gamma peak, and the total gamma activity by integrating the whole gamma spectrum starting from 480 keV (Fig. 13). It was thus decided that also the data relating to the total gamma activity should be collected as they might be valuable for the purpose of checking the main measurements.

(*) The procedures followed in the measurements are described in Appendix II.

The measurement time was varied from one rod to another so as to have a statistics of about 100,000 counts for La-140 activity each time. The number of counts relating to the total gamma activity was about 15 times higher.

The rods were monitored about 167 cm from the bottom of the rod, corresponding to the maximum axial flux level (upper level), so as to reduce counting times (Fig. 14). At the same time, this point was far enough from the control rod insertion level (approximately 70 cm) to have practically no disturbance from the control rods.

Burn-up conditions were optimized to perform a measurement undisturbed by control rods. However, since fuel rod activation, even though very low, could be measured at control rod level, it was deemed advisable to perform gamma scanning at a lower level (about 52 cm from the bottom) in order to ascertain the experimental power distribution also with the control rods in.

The data relating to each rod were immediately processed and checked in order to establish whether the measurement was to be repeated before the rod was reinserted in the fuel element, and consequently to avoid handling the rods more than once.

The check consisted in:

- (1) verifying the constancy of the ratio between the data supplied by the two counting chains;
- (2) comparing the ratio of the La-140 activity to the total gamma activity (characteristic of each rod type) with the ratio determined on the basis of the preliminary measurements on rod samples;
- (3) checking the ratio between the experimental power value and the theoretical one obtained through the two-dimension calculation method used for the programming of this experiment.

It was also necessary to perform several measurements on symmetrical positions of the critical assembly, because the experiment was con-

ducted on the actual fuel and equipment of a power reactor rather than on an ideal critical facility. Therefore, a total of 125 rods were subjected to gamma scanning. Of these, fifteen were also given an axial scan for the purpose of checking the axial power distribution at the levels considered in the experiment.

6. Analysis of experimental results

6.1 Criticality experiments

The K_{eff} value for the critical assembly formed by seven enriched uranium elements and with all the control rods out was estimated to be 1.0109 ± 0.0050 . This value was determined on the basis of the average notch reactivity of control rods F9 and F10 (measured at notch 18 by means of the rising and falling period technique) and the calibration curve of the Garigliano reactor control rods.

Table I shows the differences in K_{eff} values obtained from the periods measured for the various configurations with the control rods at the same level.

TABLE I

Configurations		$\Delta K = K_{\text{effA}} - K_{\text{effB}}$ pcm	$\pm \epsilon$ pcm	Control rod position (notch)		
A	B			F9	F10	Remainder
II	I	246.1	4.9	17	17	35
III	I	229.7	5.2	17	17	35
V	I	189.4	4.5	17	17	35
III	II	- 16.5	4.1	17	17	35
IV	II	149.7	3.6	16	16	35
V	II	- 41.2	4.4	16	16	35
V	II	- 56.7	3.0	17	17	35
V	II	- 46.3	4.1	17	16	35
V	III	- 33.6	5.0	16	16	35
V	III	- 40.2	3.4	17	16	35
V	IV	- 194.2	24.4	16	15	35
V	IV	- 190.9	5.6	16	16	35

In determining the "mean square error" of period measurements, consideration was given to:

- a) uncertainties due to defective point alignment on the charts because of incorrect change of scale or other equipment defects;
- b) intrinsic error dependent on the "waiting time". The waiting time was determined so as to obtain an error of about 1%, and at any rate not higher than 5%.

The mean square error does not include possible systematic effects nor other causes of errors that could not be investigated. One of them is the core temperature variation during the experiment, because this was controlled at the unloading system inlet and outlet and not by means of a thermocouple inside the core. At any rate, since the channel was completely flooded during the experiment and the water was continuously recirculated, it is reasonable to assume that the temperature readings were correct.

Besides, in order to shorten the measurement time, no effort was made to respect the original position of the U-235 elements during the experiment, and a change in position was allowed among those that were of minor neutron importance. This could cause a reactivity variation due to imperfect fuel homogeneity.

During plant startup tests, fuel uniformity tests were performed, which showed that the mean square error connected to this effect is $0.53 \times 10^{-4} \Delta K/K$. As it is reasonable to believe that the uniformity of the new fuel batch is equal to that of the first core load, the above figure may well be assumed as the contribution of fuel disuniformity.

The ΔK measured between the II and III configurations was slightly higher than the mean square error; it is difficult to ascertain whether the resulting ΔK is due to the worth reduction control rod F9 owing to the effect of the Pu fuel element, or whether it represents the error due to non-reproducibility of the measurement.

The K_{eff} of the 3x3 configuration with all the control rods out was estimated equal to 1.00560 ± 0.00050 by the same procedure as described above.

6.2 Power distributions

6.2.1 Level not affected by the control rods

The La-140 counting rates were corrected for the background and for the activity of the fuel rods before irradiation. The background radiation was checked every twelve hours. The activity of the fresh fuel rods was evaluated from measurements performed on the three specimens prior to their irradiation.

The counting rates were all brought back to the reference time (14 days after irradiation) by using the Ba-La chain decay law obtained from periodical scanning of the three rod specimens over the whole duration of the experiment. The resulting decay law is an exponential with a half-life of 12.6 days versus the figure of 12.8 days given in the literature.

The two sets of fuel rod data obtained from the two counting chains were appropriately normalized one to the other and averaged. The La-140 radioactivity thus obtained was converted into power density by means of the conversion factors evaluated for each rod on the basis of the macroscopic fission cross-sections of the individual isotopes and the related fission yields (Appendix III). The cross-sections were obtained with the calculation method used for the programming of the experiment. On the basis of the experimental distributions of σ_f^9/σ_f^5 measured at Winfrith⁽¹⁾, it was possible to ascertain that the calculation method assesses this ratio within $\pm 5\%$. Therefore, the error committed in passing from La-140 activity to power density is, at the most, 0.2%, in the worst case (rods enriched to 0.74% in fissile Pu). This error is negligible. In addition the fission cross-sections are the same as those in the calculation method used for the theoretical-experimental comparison; for this reason, the error was not taken into account in assessing the precision of the experimental data.

At this level, the 3x3 configuration is characterized by a diagonal symmetry due to the influence of the neutron source.

In giving the experimental distribution of the power densities (Fig. 15), the data relating to each set of symmetrical positions were averaged. The values indicated in Fig. 15 are affected by a standard deviation of $\pm 0.7\%$, which includes the random error, the error associated with the correction for decay and the error due to engineering tolerances.

The random error was evaluated from the scattering of the counting rates attained for each rod by the two measurement chains ($\sigma = \pm 0.2\%$). The standard deviation related to the best fitting of the exponential function to the decay data of the three rod specimens, net of the statistical component, represents the contribution to the error for the decay correction ($\sigma = 0.4\%$).

The scattering of the values related to symmetrical positions in respect of their average gave a standard deviation of $\pm 0.5\%$, net of the statistical fluctuations. This value represents the effect of irregularities within the manufacturing tolerances on the power density; these irregularities may involve mainly the density of the fuel and its fissile content, or the lattice pitch of the rods.

The power densities obtained from the La-140 activity measurements were checked through comparison with the corresponding values derived from processing of the total gamma activity data. The procedure is described in Appendix IV, Paragraph 1.

The comparison confirmed the power density values obtained from the La-140 activity measurements; the standard deviation between the two experimental power density distributions was $\pm 0.64\%$.

The analysis of the data relating to axial scans indicated that the perturbation due to partially inserted control rods is practically nil at the level in question.

6.2.2 Level influenced by the control rods

At this level, the gamma activity of the fuel rods proved to be very low because of the high depression in the neutron flux caused by the control rod bank. As a result, in this case the combined contribution of the natural background and rod activity prior to irradiation--the latter being quite negligible at the upper level--represents a substantial component of the total activity. Consequently, there is an appreciable increase in the uncertainty degree (σ) of these data not only due to the small number of counts, but also due to an incomplete knowledge of the activity of the individual rods prior to irradiation. In fact, for mainly practical reasons, the background evaluation of each individual rod was merely based on the extrapolation of the data measured in the specimens of three rod types.

Measurements of non-irradiated specimens indicated a strong variation in the total gamma activity from one rod type to the other, but it is thought that said activity may vary, though less remarkably, also in rods of the same type, especially in the plutonium ones.

The La-140 data are affected by a statistical error greater than that of the total gamma activity, because the related counts represent only a portion of the whole spectrum. Nevertheless, the power density values obtained from La-140 appear to be more promising since the component of the activity due to the natural and rod background is much less important than in the case of the total gamma activity. In less activated rods, which are closer to control rods and to the reflector, this component amounts to 65% of the total gamma activity versus 30% of the La-140 one. Moreover, it is justified to assume that fluctuations in the background component of rods of the same kind are negligible when only the activity of La-140 is considered. These fluctuations are probably due to traces of fission products present in the plutonium as reprocessing residues; the gamma activity of these fission products does not interfere with the 1.6 MeV activity of La-140.

The experimental data were processed as described in Appendix IV, Paragraph 2. The analysis showed a systematic discrepancy between the values of the La-140 gamma activity and those of the total activity; on the basis of the aforesaid considerations this discrepancy appears to be mainly due to the uncertainty in the total gamma activity data resulting from the strong component of the rod background.

Fig. 16 shows only the power distribution obtained from processing the La-140 activity data by a similar procedure to that described in Paragraph 6.2.1. The statistical error of these measurements is estimated to be 2.5%, net of the error relating to the background, for the determination of which sufficient elements are not available.

The other error components, such as those associated with the decay law and manufacturing irregularities, are distinctly smaller than the two preceding errors and are therefore negligible.

An indication of the total error affecting these experimental data can be provided by the standard deviation between the values of power densities from the total gamma activity and those derived from the gamma activity of La-140, after normalization, that is, $\pm 8.3\%$.

6.2.3 Fine-structure effects

A number of interesting, fine-structure effects were observed as a result of carrying out the experiment on actual reactor fuel and hardware rather than on ideal critical facilities. With regard to axial power distribution, they included:

- a) The depression ($\sim 4\%$) noticed in all the fuel rods not adjacent to the spacer-capturing rod, due to the steel spacer grids (Fig. 14).
- b) Slightly pronounced peaks ($\sim 4\%$) (Fig. 14) present only in the rods adjacent to the plutonium spacer-capturing rod; these peaks are caused by a thermal flux rise in the Zircaloy end connectors. The effect is not visible in enriched-uranium spacer-capturing rods where the thermal flux increase in the end connectors is probably smaller and is compensated by the absorption in the grids.

In the radial power distribution, the following was observed:

- c) The effect on rod power densities due to rod manufacturing tolerances. This effect was evaluated by comparison of a significant number of symmetrical rods. The value obtained (average: $\pm 0.5\%$) is net of the standard deviation of the measurement.
- d) Strong effect of the neutron source on the power level of the corner rod adjacent to the source (about a 15% local reduction) (Fig. 15).
- e) Power depressions in the peripheral fuel rods closest to the aluminium dummy assemblies (Fig. 15).

7. Comparison between the experimental data and the calculated values

7.1 Theoretical models

The K_{eff} and power distribution of the critical assemblies was estimated with the standard technique that ENEL uses, among the other, for the design of plutonium elements. This technique is based on the combination of the 5-group RIBOT⁽²⁾ and SQUID⁽³⁾ codes (with energy cut-off at 0.2 eV, 0.625 eV, 5.53 keV and 183 keV), already checked by ENEL on experimental power distributions of other critical assemblies⁽¹⁾.

The RIBOT code, developed by CNEN, performs a cell calculation for each type of fuel element rod, and provides 5-group lattice constants. For

the bidimensional diffusion calculations, use is made of the SQUID code which is characterized by a complete matrix of transfer cross-sections. The RIBOT-SQUID system, characterized by the division of the neutron thermal range in two groups, permits a more accurate representation of the events affecting the thermal component of the neutron spectrum, since it can take into account the thermal spectrum changes near the water gap or near the contact areas between uranium and plutonium fuel rods. In addition, the use of three fast groups permits a better evaluation of neutron leakage. This is of special importance when the K_{eff} of small critical assemblies is to be estimated.

The comparison was extended also to a more widespread calculation technique, such as the one based on the FORM⁽⁴⁾ and THERMOS⁽⁵⁾ codes. Here again, the bidimensional diffusion code was SQUID with three neutron groups, of which only one was thermal (energy cut-offs at 5.53 keV and 0.625 eV).

In the core representation at least three meshes were used for each lattice cell of the fuel element.

The calculations were performed on the basis of the average fuel density and fissile content for each type of rod. However, in order to ascertain the effect of variations of these quantities on the power distribution, a calculation was performed for the plutonium element, the actual values of which were certified. The results were compared with the power densities derived from the average values; the variations were small, being on the same order as was obtained from the comparison of the power densities measured on symmetrical rods.

The lattice constants of materials not forming the fuel cells were calculated with the GGC II⁽⁶⁾.

In the diffusion calculations, the control rods were represented by special parameters, i.e. absorption cross-sections for fast and epithermal energy groups, and extrapolation lengths applied to the external surface of the rod sheath for the thermal groups. The area where the rod blades intersect was represented by the lattice constants of steel-water mixture.

The most suitable calculation method to obtain the control rod parameters is on the transport theory. For this purpose, the one-dimension DTK code⁽⁷⁾ was applied to a slab model by utilizing a library with 18 energy groups (four of which are thermal) prepared by means of the GGC-II code. The control rod is represented by two homogeneous regions, the first of which is constituted by the steel-clad boron carbide rods and by the cooling water, and the second by the control rod sheath. The fuel is also subdivided into two regions, of which the peripheral one corresponds to the less enriched rods (Fig. 17b).

From the calculation with the DTK code the control rod neutron absorptions were obtained for the various energy groups. By employing the same geometrical model used in the transport code, this calculation was repeated with a diffusion code (SQUID), in which guess values were used as representative parameters of the control rods. By means of iterative calculations it was possible to establish the values of the parameters that used in the diffusion theory give the same neutron absorptions as provided by the transport theory.

The calculations with the SQUID code were performed with three and five neutron groups in order to obtain the parameters to be employed with the FORM-THERMOS-SQUID technique and with the RIBOT-5-SQUID technique, respectively.

The calculations were performed for the uranium and plutonium fuel elements in zirconium or steel channels, adjacent to a control rod. It was observed that the different fissile material content (uranium or plutonium) of the fuel elements adjacent to the control rods affects the parameters representing the control rod, whereas the effect of the channel material (zirconium or steel) can be considered negligible.

7.2 Consistency of the experimental and theoretical data

7.2.1 Criticality evaluations

Table II shows the K_{eff} values calculated for the various fuel element configurations and in the assumption of fully withdrawn control rods, together with the values derived from the experimental results.

Consistency with the experimental data appears to be satisfactory for both calculation methods.

TABLE II

Configuration	Experimental K_{eff}	K_{eff} from RIBOT-5-SQUID	K_{eff} from FORM-THERMOS-SQUID
I	1.01090 \pm 0.00050	1.00800	1.01560
II - III	1.01328 \pm 0.00050	1.01070	-
IV	1.01486 \pm 0.00050	1.01375	1.02140
V	1.01280 \pm 0.00050	1.01130	-
3x3	1.00560 \pm 0.00050	1.00600	1.00900

A more stringent check is provided by the comparison of the ΔK values arising from replacement of an enriched-uranium element with a plutonium element in the all-uranium configuration (Table III).

TABLE III

	Experimental ΔK	ΔK from RIBOT-5-SQUID	ΔK from FORM-THERMOS-SQUID	ΔK from RIBOT-5 ^(R) -SQUID
$\Delta K_{\text{II/III-I}}$, pcm	238 \pm 9	270	-	210
$\Delta K_{\text{IV-I}}$, pcm	388 \pm 70	575	580	445
$\Delta K_{\text{V-I}}$, pcm	191 \pm 7	330	-	267

R = revised library

This comparison evidences a tendency of both calculation methods to overestimate the ΔK resulting from the replacement of one enriched-uranium element with a plutonium element. The overestimate is less appreciable when the replacement is made in a corner position of the configuration.

The fact that this tendency is common to both calculation methods, notwithstanding the different number of neutron groups, might indicate an overrating of the Pu-239 multiplication properties provided by the code libraries.

The calculations were repeated with a reduced epithermal fission integral of Pu-239 of the RIBOT-5 library from 338 to 293 barns according to a recent code revision⁽⁸⁾. The related results shown in the last column of Table III are in good agreement with the experimental values.

7.2.2 Power distributions

The power distributions relating to the two gamma scanning levels were calculated with both techniques described above, that is, one based on the RIBOT-SQUID system and the other based on the FORM-THERMOS-SQUID system.

Figs 18 and 19 show the percentage deviation between the calculated and experimental values of the power distributions for the level without control rods.

The results of the two calculation techniques are fairly consistent with the experimental data ($\sigma < \pm 2\%$), more significant deviations being observed on the rods at the border of fuel areas having very different characteristics. The values obtained for the corner rods with the FORM-THERMOS-SQUID technique show a systematic deviation in respect of the experimental data. This deviation cannot be found in the results obtained with the first calculation method because of the adoption of the two thermal groups.

At the level characterized by the presence of control rods, the deviations between the theoretical and experimental values are greater, as evi-

denced in Fig. 16, which provides a comparison between the experimental power distribution and the theoretical one calculated with the RIBOT-SQUID method. The values obtained with the FORM-THERMOS-SQUID system are not indicated as they do not differ substantially from those obtained with the preceding method.

Because of the great uncertainty by which the experimental data are affected, it is practically impossible to perform an analysis of the errors due to the calculation method. However, from Fig. 16 it can be noted that the deviations are distributed in a systematic pattern, the largest occurring in the fuel rods adjacent to the control rods, with opposite signs on the two sides. This trend may be due to off-center positioning of the control rods, which is actually possible also because of the 5-mm clearance between the control rod and the fuel sheath.

To confirm this assumption a theoretical evaluation of this effect was performed with the transport code DTK for a control rod in the farthest off-center position, that is, with one blade leaning completely on the sheath of one fuel element (Fig. 17 a).

On the fuel cells closest to the control rods, the effect determined a variation of about +14%, that is, consistent with the value deduced from the deviation between theoretical and experimental values.

On the basis of the above considerations it seems that, at the time of the experiment, control rods E10, F10 and F9 were all positioned more or less eccentrically.

By applying the eccentricity correction factors derivable from Fig. 17 to the theoretical power distribution, a standard deviation equal to +5% is obtained which does not seem large in the light of the uncertainty on the actual control rod position and the measurement data.

8. Conclusions

The information provided by the criticality experiments in the Garigliano reactor usefully supplement the experimental data available for the design of plutonium fuel elements. For these experiments, prototype plutonium elements were designed and used as normal reload fuel in the Garigliano nuclear power station. Thus the resulting data differ from those of similar experiments in that they include:

- power density distributions associated with highly heterogeneous lattices (three or four enrichments per fuel element, water gap, presence of control rods);
- reactivity variations following replacement of enriched-uranium elements with plutonium elements.

These experimental data are satisfactorily accurate. The technique used for power density measurements (gamma activity scanning by means of a NaI crystal) proved its outstanding capabilities and its extreme effectiveness, because it revealed minor differences in power density, such as those due to the manufacturing tolerances.

The good agreement between the experimental values and those obtained with the calculation methods adopted by ENEL (RIBOT 5 - SQUID and FORMTHERMOS-SQUID), already observed in previous criticality experiments, was fully confirmed in this case. The power density was calculated with a standard deviation less than 2%, and reactivity with an error below 0.5%.

BIBLIOGRAPHY

1. A. Ariemma, G. Lesnoni La Parola, M. Paoletti Gualandi, P. Peroni, B. Zaffiro: "Accuracy of Power Distribution Calculation Methods for Uranium and Plutonium Lattices Based on Recent Experiments and ENEL Reactor Operation Data". ANS International Conference, Washington, 11-13 November 1968.
2. G. Buffoni, P. Loizzo, S. Lopez, M. Petilli: "Burn-up of Pressurized or Boiling Water Reactors". Symposium on "Advances of Reactor Theory", Karlsruhe, 27-29 June 1966.
3. A. Daneri, B. Gabutti, E. Salina: "SQUID-360, A multigroup Diffusion Program with Criticality Searches for the IBM-360". EUR 3882, 1968. EURATOM.
4. D. J. Mc Goff: "FORM, a Fourier Transform Fast Spectrum Code for IBM-709". NAA-SR-Memo 5766, September 1960. Atomic International.
5. H. C. Honek: "THERMOS, a Thermalization Transport Theory Code for Reactor Lattice Calculations". B. N. L. -5826. Brookhaven National Laboratory.
6. C. V. Smith, H. A. Vieweg: "G.G.C. II, a Program for Using the GAM II and GATHER II Spectrum Codes in Preparing Multigroup Cross-section Input on Punched Cards for the GAZE, GAZED, DSN, CAPLSN, 2 DXY, TDC, GAMBLE, FEVER and GAD Codes". G. A. -4436, December 1963. General Atomic.
7. "DTK Operating Instructions", Los Alamos.
8. P. Loizzo: "A Physical Model for Light Water Lattice Calculations". BNWL-753, February 1968. Battelle North West Laboratory.

APPENDIX I

PRELIMINARY MEASUREMENTS TO SET DOWN OF THE TECHNIQUE FOR GAMMA SCANNING OF Pu FUEL RODS

The purpose of the preliminary measurements was to:

- a) Test the equipment.
- b) Determine the variation of the fission product spectra with time.
- c) Determine the irradiation and decay times; neutron flux levels; doses to the personnel handling the elements.
- e) Train the personnel destined to perform the measurements on the fuel elements.

Six fuel rod specimens were purposely procured to perform the preliminary measurements; their isotopic compositions were:

- Two specimens with 0.74% of fissile Pu (Pu- A type)
- Two specimens with 2.855% of fissile Pu (Pu- C type)
- Two specimens of 2.41% enriched uranium (U).

These specimens are 15 cm long and have the same structural characteristics as those of the plutonium and enriched uranium fuel elements shown in Fig. 20.

The six specimens were divided in two sets of three specimens each. The first set was used for the preliminary measurements, while the second was to be used to check the decay laws of the gamma activity during rod scanning and was therefore to be irradiated together with the fuel elements.

1. Measurement program

The measurement program was divided into the following three phases:

- a) Measurement of the neutron fluxes in the irradiation channel.
- b) Adjustment of the measurement system and specimen irradiation.
- c) Measurements proper.

Copper disk monitors 9 mm in diameter and 2 mm thick were used for the thermal neutron flux measurements; the monitors were always irradiated in pairs and one or two of them were covered with a cadmium layer in order to obtain the thermal flux and epithermal component.

After irradiation, the monitors were subjected to counting by means of a 2"x2" photoscintillator and a multichannel analyzer. The detection system was calibrated by using the 511-keV peak of a Na²² source calibrated at 2%.

Besides, by means of a tungsten wire and later of a copper wire, the neutron flux distribution was measured along the channel provided for the irradiation of the three specimens. This channel, which is normally used to insert a neutron counter as a reactor control instrument, crosses the main biological shield transversally until it nearby reaches the gap between the shield and pressure vessel in correspondence of the core mid-plane, and then it returns to the center of the shield. In the zone in front of the core a certain length of the channel is enclosed by a lead sleeve.

Fig. 21 shows the neutron flux distribution in this channel; it can be noted that the only section with an acceptable flux rate is that included between a depth of 11.5 and 12.5 m: this is the section used for the irradiation of the rod specimens.

The second phase included calibration of the two detection chains and a first adjustment of the measurement technique. Subsequently, one each of the three specimen types were irradiated together with the flux monitors. Each rod specimen was irradiated for 60'.

The neutron fluxes and cadmium ratios for the three specimens are the following:

	ϕ , n/cm ² sec	RC
U specimen	5.0×10^9	6.4
Pu specimen- A type	3.1×10^9	4.4
Pu specimen- C type	2.7×10^9	3.6

The day after irradiation, the fission product distribution was measured along the three specimens by means of a detection system provided with a 3 mm slit. Distribution was rather uniform in the central part of the specimens. Finally, the specimens were inserted in one of the aluminum guide tubes provided for the fuel element rods.

The third phase included:

- a) Measurement of the background radiation spectra of the three specimens at different times.
- b) Measurement of the radiation level on the aluminum guide tube in correspondence of the specimens.

2. Description of the gamma spectra measurements

The measurement technique of the gamma radiation spectra is the following:

- a) For the counting, the aluminum tube was positioned in succession at notches corresponding to the specimen positions.
- b) The analyzer was calibrated on 400 channels, (bias at 200 keV) (*), corresponding to 5 keV/channel.
- c) For the gross-gamma measurements, the peak at about 480 keV was taken as reference and the integral was extended from the 10th channel preceding the peak to the remainder of the spectrum.
- d) Since the 480-keV reference peak was not always symmetrical in respect of a given channel, correction was made by means of a computer program which determines the fraction of counts pertinent to the 10th channel, to be added in the integral.
- e) The 1.6-MeV La-140 peak occurred between channels 268 and 272; by operating the amplifier it was possible to keep the peak within these limits, except for few days. At any rate, it was experimentally demonstrated that even when the peak moved to channel 277, the integral was constant, at least within measurement errors.

(*) between 0.2 and 2.2 MeV

Integration was performed on 40 channels, selecting the first and the last one across the peak so that their connecting line was horizontal; when this was not possible, two adjacent integrals were averaged so that the lines connecting the extreme channels crossed each other with opposite inclinations.

- f) The background radiation was measured first with the non-irradiated specimens in front of the collimator and later without the specimens; subsequently, the background radiation was measured every day without the specimens. The difference between the two first measurements represents the contribution of the non-irradiated uranium and plutonium to the background and must be subtracted from all the spectra; the daily measurements indicate the contribution of the external radiation or background proper, which has to be subtracted from each spectrum.

3. Measurement results

3.1 Radiation levels

Figure 22 shows the curve of the radiation level, as a function of time, normalized to a thermal flux of 1×10^9 n/cm² sec for the capsule with the highest activity, that is, the type C plutonium capsule with 2.855% of fissile Pu.

On the basis of the results in Fig. 22, in order to estimate the radiation level on the upper part of the fuel element to be disassembled and re-assembled for rod gamma scanning, it was necessary to make some empirical-theoretical assumptions. In fact, because of the complicated geometry and poor accessibility to the measurement points, it was only possible to estimate the order of magnitude of the radiation levels.

An extrapolation was attempted on the basis of the following data:

- a) A level of about 1 mRem/h was measured on the surface of the non-irradiated capsules.
- b) After 15 days' decay, about 10 mRem/h were measured on the surface of the non-irradiated capsules.

- c) A radiation level of 5 mRem/h was measured in contact at mid-height of the non-irradiated fuel elements, stored in the measurement room, and 0.5 mRem/h in the upper part.
- d) By means of a simple proportion it was possible near mid-height of the irradiated fuel element after 15 days' decay to foresee a dose of 50 mRem/h and of 5 mRem/h on the head. These doses are sufficiently low to allow the disassembly and re-assembly of the fuel elements.

3.2 Gamma spectrometry measurements

Table 4 summarizes the results of the gamma spectrometry measurements for the period comprised within the 15th and 30th day from irradiation.

Column I shows the number of filed spectra; column 2, divided in three parts, gives the date, time of measurement and the hours elapsed between irradiation and the measurements; column 3, also divided in three parts, one for each capsule, shows the gross-gamma integral, expressed in pulses/second, net of the background and of the natural activity of the specimen; column 4, divided in three parts, shows the integral on the La peak, expressed in pulses/sec, net of the background and natural activity of the rods; column 5 shows the time function $f(t)$ for the La-140 decay.

4. Analysis of the results

4.1 Measurements of the total gamma activity

On the basis of the information provided in the literature, an effort was made to find an analytical formula which would show the gross gamma results (C) in the form:

$$C = A t^{-B}$$

where A is a constant dependent on neutron flux, macroscopic fission cross-section, detector efficiency and source geometry

B is a constant dependent only on the type of fuel analyzed.

TABLE IV

ANALYSIS OF SPECTRA - CHAIN I

(Values of integrals in cps)

N. Spectrum	DATE			GROSS-GAMMA INTEGR.			¹⁴⁰ La INTEGR.			f(r)
	Day	Hour	$\Delta T, h$	U	Pu "A"	Pu "C"	U	Pu "A"	Pu "C"	
16	27-5	16,30	335,0	1170,5	770,5	1547,3	95,7	57,4	113,1	0,4667
17	28	9,30	352,0	1110,6	715,7	1447,8	93,0	55,0	108,0	0,4498
18	28	16,00	358,5	1091,7	703,7	1413,7	90,7	54,4	107,0	0,4434
19	29	10,30	377,0	1022,7	667,2	1332,4	86,8	52,3	100,4	0,4258
20	29	16,00	382,5	1010,2	656,0	1310,6	85,75	51,4	100,6	0,4207
21	30	10,30	401,0	953,1	620,5	1232,9	82,0	49,0	96,1	0,4037
22	30	17,00	407,5	949,2	614,4	1214,5	81,8	49,1	95,0	0,3980
23	31	10,00	424,5	898,1	584,1	1157,8	77,7	47,4	91,5	0,3833
24	31	16,00	430,5	884,9	574,5	1138,6	76,7	46,0	90,2	0,3781
25	1-6	11,30	450,0	836,2	548,7	1046,6	73,1	44,5	85,7	0,3620
26	2	11,00	473,5	796,3	506,4	1018,1	70,05	41,2	80,5	0,3434
27	3	10,00	496,5	758,7	484,5	964,4	66,2	39,96	77,2	0,32616
28	3	16,30	503,0	748,9	478,8	948,6	65,8	39,0	76,4	0,3214
29	4	10,00	520,5	714,5	462,4	910,1	62,3	38,4	73,0	0,3093
30	4	16,00	526,5	703,1	455,7	896,2	60,8	37,0	72,2	0,30475
31	5	17,30	552,0	672,2	429,6	852,8	58,9	35,3	68,1	0,2878
32	6	11,00	569,5	649,7	412,8	821,0	56,8	33,7	65,5	0,2733
33	6	16,30	575,0	643,7	406,3	810,3	56,3	33,3	64,7	0,2733
34	7	10,00	592,5	613,8	399,4	783,3	53,5	32,2	62,8	0,2627
35	7	16,30	599,0	610,2	394,6	774,2	52,8	31,5	62,2	0,2589
36	8	11,00	617,5	591,2	377,8	746,4	50,45	30,1	58,8	0,2484
37	9	10,30	641,0	568,1	357,0	712,9	48,1	28,3	56,0	0,2355
38	10	10,00	664,5	535,2	347,0	682,3	45,0	26,9	53,3	0,2234
39	10	16,30	671,0	528,5	345,7	675,6	44,1	26,95	52,6	0,2201
40	11	9,30	688,0	516,5	332,8	654,3	43,0	25,95	50,1	0,2119
41	11	16,30	695,0	509,1	327,6	645,5	42,3	25,6	49,9	0,20855
42	12	10,00	712,5	497,2	319,6	623,0	41,4	24,6	47,60	0,20044
43	12	16,00	718,5	493,3	315,2	622,8	40,24	24,18	47,23	0,19775
44	13	11,30	739,0	475,0	304,6	599,0	38,8	22,9	44,8	0,18865
45	14	11,00	762,5	453,9	291,9	578,6	36,27	21,87	42,74	0,17908

For the three types of fuel, the following different expressions were found:

$$\begin{array}{ll} \text{U} & C = 890,000 t^{-1.1401} \\ \text{Pu-type A} & C = 654,460 t^{-1.1610} \\ \text{Pu-type C} & C = 1,532,000 t^{-1.1876} \end{array}$$

The decay time, within which these expressions are effective, is included between the 15th and 30th day, but it can be extrapolated for a few days exceeding this period.

The differences between the theoretical values obtained by means of the aforesaid formula and the experimental ones are shown in Table 5, as a function of the decay time.

It can be noted that, notwithstanding the overall compensation between the negative and positive deviations, the distribution appears to indicate a discrepancy between the analytical expression and the experimental results.

4.2 Measurement of the La-140 activity

Use was made of the data in Table 5 relating to the period between the 15th and 30th day of decay, to determine the apparent half-life of the three analyzed fuels. The values obtained are the following:

$$\begin{array}{ll} \text{U} & T_{1/2} = 12.79 \text{ d} \pm 1\% \\ \text{Pu-type A} & T_{1/2} = 12.78 \text{ d} \pm 1\% \\ \text{Pu-type C} & T_{1/2} = 12.79 \text{ d} \pm 1\% \end{array}$$

The deviation of the half-life from the figure of 12.8 days given in literature is within the experimental error.

The deviations between the theoretical and experimental values are given in Table 5 as a function of the decay time. The standard deviation referred to a 95% confidence level is comprised between:

- 0.64 and 1.08% for uranium
- 0.63 and 1.06% for type A plutonium
- 0.55 and 0.92% for type C plutonium.

TABLE V

PERCENTAGE DEVIATIONS BETWEEN CALCULATED AND EXPERIMENTAL VALUES

N. Spectrum	$\Delta T, h$	GROSS GAMMA			140 La		
		U	Pu "A"	Pu "C"	U	Pu "A"	Pu "C"
16	335,0	0,57	-0,53	-0,60	-0,59	-0,52	-1,73
17	352,0	0,17	1,09	0,10	-1,43	0,06	-0,79
18	358,5	0,19	0,65	0,30	-0,35	-0,27	-1,30
19	377,0	0,59	0,15	0,20	-	-0,38	0,02
20	382,5	9,20	0,15	0,10	-	0,14	-0,38
21	401,0	0,60	0,24	0,70	0,35	0,79	0,06
22	407,5	-0,82	-0,66	0,20	-0,82	-0,83	-0,20
23	424,5	0,06	-0,33	0,20	0,55	-1,07	-0,21
24	430,5	-0,06	-0,30	0,20	0,48	0,56	-0,15
25	450,0	0,55	-0,86	-	0,93	-0,47	0,61
26	473,5	-0,37	1,25	0,10	-0,07	1,94	1,58
27	496,5	-0,94	0,19	0,10	0,42	0,13	0,63
28	503,0	-1,12	-0,15	-	-0,43	0,82	0,20
29	520,5	-0,31	-0,72	-	1,18	-1,47	0,91
30	526,5	-0,01	-0,51	0,20	2,12	0,76	0,54
31	552,0	-0,92	-0,09	-0,30	-0,40	-0,24	0,66
32	569,5	-1,07	0,27	-0,20	-0,70	0,45	0,62
33	575,0	-1,24	0,73	-0,10	-1,06	0,41	0,61
34	592,5	0,10	-1,04	-0,30	0,08	-0,18	-0,35
35	599,0	-0,56	-1,10	-0,40	-0,05	0,55	-0,85
36	617,5	-0,85	-0,27	-0,30	0,36	0,96	0,62
37	641,0	-1,14	1,05	-0,20	-0,20	1,78	0,17
38	664,5	0,72	-0,29	-0,10	1,17	1,58	-0,16
39	671,0	1,53	-0,35	0,40	1,70	-0,07	-0,32
40	688,0	0,33	-0,15	-	0,44	-0,09	0,74
41	695,0	0,61	0,27	-	0,49	-0,32	-0,44
42	712,5	0,14	-0,16	0,60	-0,59	-0,30	0,30
43	718,5	-0,02	0,25	-0,20	0,17	0,06	-0,26
44	739,0	0,54	0,42	0,20	-0,79	0,89	-0,41
45	762,5	1,52	1,02	-	0,63	0,18	-0,19
negative deviations		14 (-)	16 (-)	11 (-)	13 (-)	14 (-)	14 (-)
zero deviations				5 (o)	2 (o)		
positive deviations		16 (+)	14 (+)	13 (+)	15 (+)	16 (+)	16 (+)

It follows that, in this time interval, the 1.6-MeV lanthanum peak can be reduced to a common time for the various types of fuel with the theoretical function $f(t)$.

5. Conclusions

- a) The equipment provided for the measurement proved adequate provided that the room temperature remained within the acceptable limits (20-25 °C).
- b) A maximum flux of 5×10^9 at the fuel element scan level and a one-hour exposure are enough to obtain good statistics in the counting of La-140 activity.
- c) The preliminary measurements suggested 15 days' decay time before starting the measurements.

APPENDIX II

DESCRIPTION OF THE MEASUREMENT AND CONTROL PROCEDURES

1. Check of the flux in the 3 x 3 critical configuration

After irradiation of the 3x3 configuration three rod specimens belonging to the second set and the copper monitors with and without cadmium for the measurement of rod irradiation were removed from the dummy element located near the critical assembly.

The copper monitors were subjected to counting according to the technique described in Appendix 1, and the resulting heat fluxes were:

$$\begin{array}{l} 1.34 \times 10^9 \text{ n/cm}^2/\text{sec.} \\ 1.24 \times 10^9 \quad \text{"} \\ 1.7 \times 10^9 \quad \text{"} \\ 1.4 \times 10^9 \quad \text{"} \end{array}$$

The average value corresponds fairly well with a maximum flux of 2.5×10^9 in the area of the critical assembly not affected by the control rods. The flux level obtained was thus considered satisfactory for the measurement.

2. Measurements on fuel rods

The measurements on fuel rods were carried out in the fresh fuel handling room. The rods were removed from the elements, inserted in aluminum sheaths and placed in the monitoring equipment. The measurements included: one measurement of the axial distribution and two measurements of the radial distribution at two elevations of interest. In addition, twice a day the background and the activity of the three reference capsules housed in a guide tube of the type used for the fuel rods were measured.

2.1 Procedure for axial distribution measurement

The procedure for this measurement was as follows:

- a) The aluminum sheaths containing the rod was located at the first upper notch (all the guide tube is marked with notches at 5 cm intervals).

- b) The threshold of the analyzer No. 2 was shifted to the 45 channel.
- c) Connection of the analyzer to the multiscaler (storage in successive memory positions of the countings related to each axial position); measuring time 10 sec.; waiting time 10 sec.; energy range 480 keV - 2.5 MeV.
- d) The rod rotation device was then actuated.
- e) All memories were brought back to zero and counting began. Rotation was stopped during the waiting time (10 sec.).
- f) The sheath was then moved to the next notch and rotation was resumed.
- g) The operation was repeated down to the end of the rod.
- h) the resulting distribution was plotted on paper.

2.2 Procedure for the radial distribution measurement at two elevation of interest

The procedure aimed at obtaining from both detector chains the plot of the fission product spectrum, the integral on the 1.6 MeV peak of La-140, and the integral over all the spectrum from above 480 keV up to 2.2 MeV, with subdivisions of approximately 5 keV/channel. The two elevations at which the measurements were taken were clearly marked on the aluminum sheaths.

The procedure was as follows:

- a) The aluminum sheath was located at the selected notch.
- b) The two analyzers were arranged, by means of the amplifier so that the first peak of the spectrum would fall in the channel 55 ± 2 and the 1.6 MeV peak in channel 280 ± 3 .
- b) On the basis of a preliminary measurement, the counting time was selected so as to have at least 25,000 pulses on the 1.6 MeV peak.
- c) The rod rotation device was started.
- d) The memory was brought back to zero and counting began.
- e) The spectrum was plotted.
- f) Integration of the 1.6 MeV peak over 40 channels with a horizontal connecting segments or with two cross segments (see Appendix 1).

- g) All the spectrum was integrated starting from 10 channels before the 480 keV peak to channel 399 (see Fig. 13).
- h) Counting and integration operations were repeated other two times.
- i) The rod identification data, the date and time (beginning and end of the measurement), the integration channels and the resulting integrals were recorded on a special form.
- e) The consistency of the values given by the two analyzers were checked before returning the rod for re-insertion in the element.

2.3 Measurement of the activity of three rod specimens and background

This procedure is quite similar to the one described in 2.2 except that the aluminum sheath contained the three rod specimens. The position of these specimens was marked on the external surface of the sheath by means of identification notches. For the background measurement, use was made of the empty part of the aluminum sheath. This procedure was repeated twice a day, at 0800 and 1600 hours. The specimen measurement time was 360 seconds and the background activity measurement time was 600 seconds.

APPENDIX III

LA-140 ACTIVITY-POWER CONVERSION FACTORS

The activity is proportional to the number of La-140 atoms, which in turn are produced in different amounts according to the fissioned isotope. Likewise, the energy generated in each fission depends on the type of isotope. Thus, we have the equation:

$$\frac{P}{A} \propto \frac{\sum_i E_i F_i}{\sum_i \gamma_i F_i}$$

where E_i , γ_i and F_i are respectively the fission energy, the number of La-140 atoms produced per fission and the number of fissions of the considered isotope.

The following table gives the values of E_i and γ_i for the isotopes present in the fuel rods.

Isotope	E_i (Mev)	γ_i La-140 (%)
U-235	194	6.25
U-238	193	5.92
Pu-239	201	5.16
Pu-241	205	6.21

With the theoretical values of F_i obtained by means of a 5-group diffusion calculation performed on the 3x3 assembly, the conversion factors for each rod of the assembly were obtained.

The analysis revealed that for a given type of rod the conversion factors are not affected by the position of the rods in the core. It is

thus sufficient to use only one factor for each rod type. The values normalized to unity in respect of the values for the 2.41% enriched-uranium rods, are given in the following table.

Element	Rod type	La-140 activity-power conversion factor
2.3% U	1.83% of U-235	1000
	2.41% of U-235	1000
Standard Pu	0.74% of fissile Pu	1139
	1.40% of fissile Pu	1172
	2.855% of fissile Pu	1200
Mixed U-Pu	1.83% of U-235	1000
	2.41% of U-235	1000
	1.80% of fissile Pu	1185
	2.89% of fissile Pu	1200

APPENDIX IV

REDUCTION OF THE TOTAL GAMMA ACTIVITY DATA TO POWER DENSITY

The procedure consisted in reducing the total gamma activity into the La-140 gamma activity by means of appropriate correlation formulae. The values thus obtained can easily be reduced to power density, and it is possible to overcome the difficulty of determining theoretically and accurately the law with which the ratio between power density and total gamma activity varies versus the composition of the fissile material and the decay time.

Two different sources of information were used for the two scanning levels to transform the total gamma activity values into La-140 activity.

1. Level not affected by the control rods

The correlation formula for this level was obtained from the data collected in the periodical scanning of the three rod specimens. In this manner, the power density values determined on the basis of the total gamma activity provide meaningful independent check of the corresponding values obtained directly from the La-140 gamma activity.

The total gamma activity values of the rod specimens are first corrected to allow for the background and rod activity prior to irradiation and are then transformed into power density by means of the following correlation formula:

$$P/A_{\gamma \text{ tot}}(N_i, t) = (B/A) t^{\alpha} (P/A_{\gamma 140})$$

where B/A and α vary with the plutonium concentration in the rods (N_i)

$P/A_{\gamma 140}$ is the factor for conversion from La-140 gamma activity to power density normalized to 1 for the U-235 rods.

The parameters B/A and α were obtained by the best fit of the $A \gamma_{140}/A \gamma_{tot}$ values measured for the three rod specimens and by extrapolation for the other rod types. $P/A \gamma_{140}$ was calculated with the method described in Appendix III. The related values are tabulated below

Rod type	B/A	α	$P/A \gamma_{140}$
1.83 & 2.41% U-235	2.6735×10^{-5}	1.1185	1
U_{nat} , 0.74% Pu_f	2.1199×10^{-5}	1.1439	1,139
U_{nat} , 1.4% Pu_f	1.9291×10^{-5}	1.1564	1,172
U_{nat} , 1.8% Pu_f	1.8588×10^{-5}	1.1618	1,185
U_{nat} , 2.85% Pu_f	1.7452×10^{-5}	1.1716	1,200

2. Level affected by the control rods

The total gamma activity of the fuel rods were transformed into power density by means of the following correlation formula:

$$P/A \gamma_{tot}(N_i, t) = \left[A \gamma_{140}(N_i, t) / A \gamma_{tot}(N_i, t) \right] e^{\lambda t} P/A \gamma_{140}$$

where the first term in the second member was derived, for each fuel rod type, by best fitting the ratios between the La-140 gamma activity and the total gamma activity obtained from the measurements at the level not affected by the control rods; λ is a decay constant related to La-140 activity ($= 2.2917 \times 10^{-3} \text{ sec}^{-1}$).

This procedure for the reduction of the total gamma activity data is based on the assumption that the ratios between La-140 gamma and total gamma activities are not appreciably affected by variations in the neutron spectrum. On the other hand, a spectrum variation from the unaffected level to the control-rod-affected level can be considered negligible.

A comparison between the power density values obtained as above with those obtained directly from the La-140 gamma activity values reveals a systematic plus difference. In the light of the considerations stated in Paragraph 6.2.2., this difference was attributed to an error in the evaluation of the background component of the total gamma

activity. On this assumption a correction was made in order to eliminate this difference throughout the measurements. The resulting percentage difference plotted as a function of the number of counts per second of the total gamma activity were distributed statistically (Fig. 23).

The figure of 2.5% can be considered the standard deviation affecting all measurements of La-140 gamma activity, because the statistical component associated with the total gamma activity measurements is negligible.

APPENDIX V

CRITICALITY TESTS IN THE REACTOR VESSEL

1. Reactor conditions prior to the tests

After removal of the pressure vessel head and turning vane, part of the fuel elements were transferred from the reactor to the pool to free an area of the reactor for the criticality tests. The fresh elements used for the tests were placed in a scattered arrangement in the reactor to avoid critical masses. Dummy elements were placed in the empty cells to support the fully inserted control rods. A map of the reactor situation is given in Fig. 4.

2. Criticality

Fig. 24 shows the reactor region in which the critical assembly was formed, the position of the neutron source and the initial positions of the instrumentation.

Neutron multiplication during loading operations was monitored by two fission chambers, denoted by numbers 10 and 11, which did not belong to the safety system, and by five compensation chambers connected to the safety system so that any one of them would be able to scram the reactor for high neutron flux (chambers 1 to 4) and for short period (chamber 7, logarithmic channel). All chambers were positioned at mid-height of the core, except for the compensation chamber No. 4, which was placed 70 cm above the mid-height to provide a reference reading during the initial control rod withdrawal stage.

The presence of a high gamma radiation background due to the other irradiated elements in the reactor created difficulties in low-level neutron flux recording by means of the compensation chambers. In fact, although these chambers had been satisfactorily tested out of the reactor, because of the high gamma background they gave no response to the neutron flux generated by one of the sources in the reactor. In some cases, the signal was even negative and became positive when the chamber was moved away from the irradiated elements.

In order to have a reliable response, the neutron/gamma ratio was increased by loading the first four elements of the minimum critical one at a time around the neutron source. Actually, it had been determined that seven elements would be required for criticality.

Under these conditions, withdrawal of the control rods close to the fuel caused a change in the compensation chamber reading that appeared to be acceptable for safe continuation of the loading operations.

During this preliminary loading stage, the gamma activity of the steel end of the control rod appeared to affect the reading considerably as it passed in front of the compensation chamber; in fact, the instrument gave a full scale reading and consequently a high-flux scram signal. To avoid this inconvenience, the compensated chambers were removed from the fuel and placed near the control rods that could remain out of the reactor throughout the tests. The final position of the chambers is shown in Fig. 4.

The fission chambers always gave a satisfactory response; however, the presence of a strong source required the fission chambers to be positioned far from the fuel elements.

On the basis of this information, other fuel elements were loaded and criticality was reached with seven elements and with the adjacent control rods withdrawn to notch 19.

The normalized inverse count rate of the chambers are given in Fig. 25.

After about thirty hours from first criticality, the measurement was repeated to check reproducibility, and the reactivity of the assembly was found to be unaltered.

Subsequently, the two highest-worth control rods (F9 and F10) were inserted in the reactor to permit complete withdrawal of the remaining rods. Under these conditions the two control rods were calibrated at a few notches to determine the K_{eff} of the seven-element assembly with all the rods out.

3. Replacement tests

The experience acquired with the minimum critical assembly permitted prompt execution of criticality measurements on the critical assembly in which a uranium element was replaced with a plutonium element in different positions.

The replacement tests were performed with an aim at obtaining at least two critical assemblies characterized by the same control rod position, in order to determine the reactivity variations associated with the replacements on the basis of the differences in period.

b	b	a	a	a	a	b	b
b	a	a	a	a	a	a	b
a	a	a	a	a	a	a	a
a	a	a	a	a	a	a	a
a	a	a	a	a	a	a	a
a	a	a	a	a	a	a	a
b	a	a	a	a	a	a	b
b	b	a	a	a	a	b	b

FIG. 1 UO_2 RELOAD FUEL ELEMENT

a = Rods enriched to 2.41% U^{235}

b = Rods enriched to 1.83% U^{235}

Average U^{235} enrichment: 2.3%

c	c	b	b	b	b	c	c
c	b	b	a	a	b	b	c
b	b	a	a	a	a	b	b
b	a	a	a	a	a	a	b
b	a	a	a	a	a	a	b
b	b	a	a	a	a	b	b
c	b	b	a	a	b	b	c
c	c	b	b	b	b	c	c

FIG. 2 STANDARD PROTOTYPE PLUTONIUM FUEL ELEMENT

a = Rods containing 2.855 wt % of fissile plutonium

b = Rods containing 1.40 wt % of fissile plutonium

c = Rods containing 0.74 wt % of fissile plutonium

Average fissile plutonium content: 1.82%

d	d	c	c	c	c	d	d
d	c	c	b	b	c	c	d
c	c	b	a	a	b	c	c
c	b	a	a	a	a	b	c
c	b	a	a	a	a	b	c
c	c	b	a	a	b	c	c
d	c	c	b	b	c	c	d
d	d	c	c	c	c	d	d

FIG. 3 MIXED URANIUM-PLUTONIUM PROTOTYPE

- a = Rods containing 2.89 wt % of fissile plutonium
 b = Rods containing 1.80% wt % of fissile plutonium
 c = Rods enriched to 2.41% U²³⁵
 d = Rods enriched to 1.83% U²³⁵

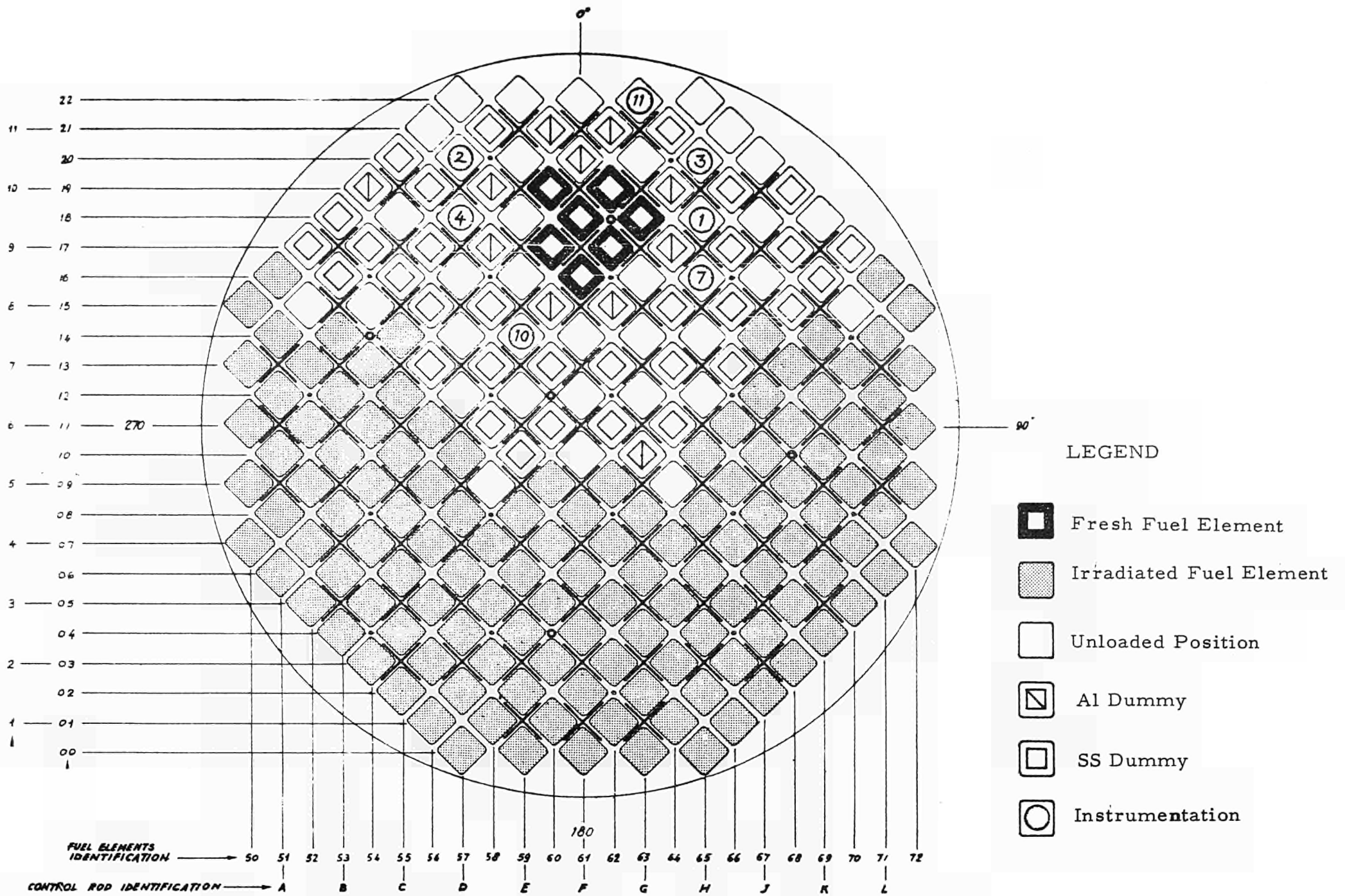


FIG. 4 - LOCATION OF THE CRITICAL ASSEMBLIES IN THE VESSEL

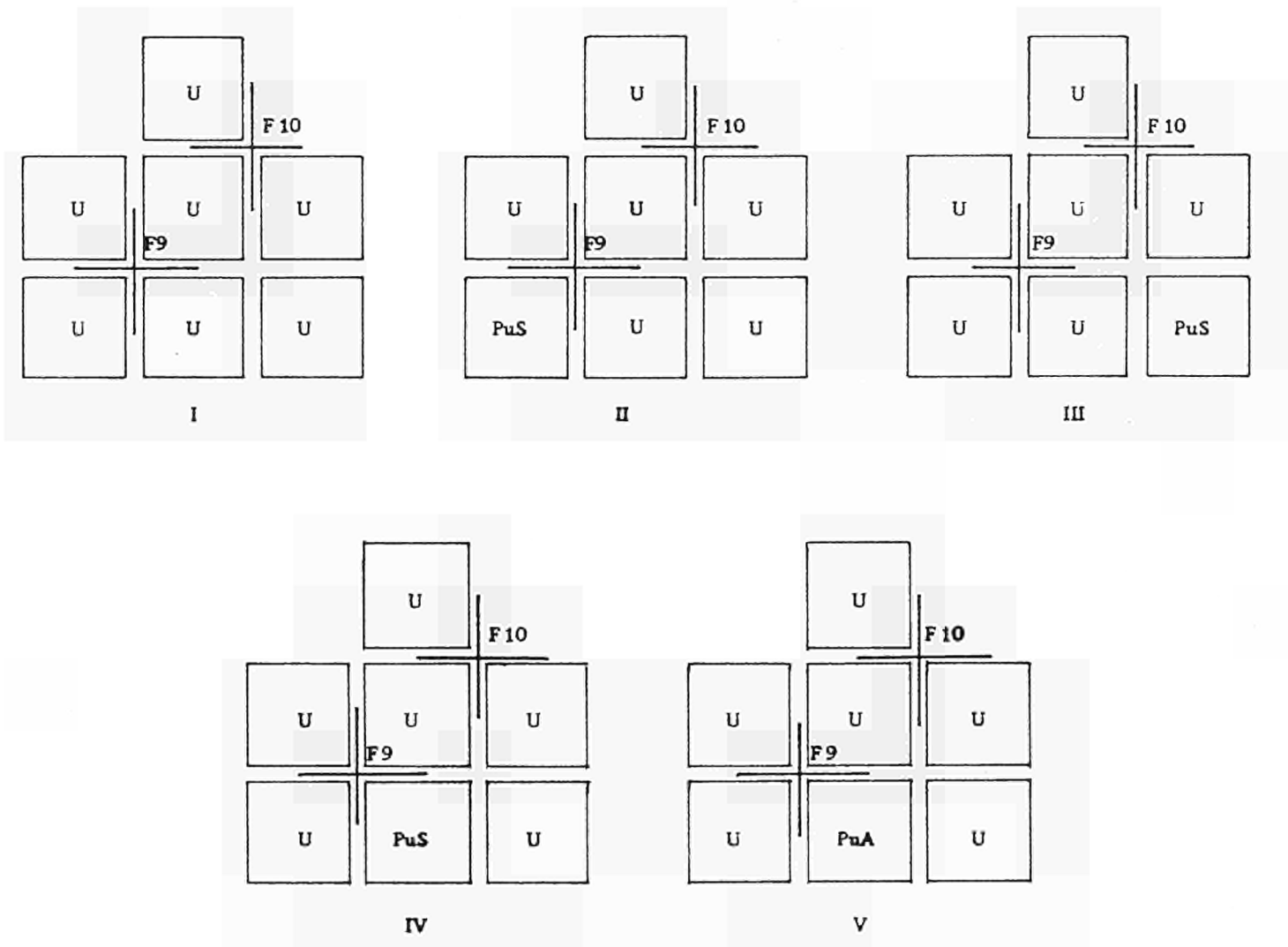
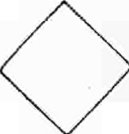








FIG. 5 - CRITICAL CONFIGURATIONS

-  Enriched uranium fuel element
-  Standard plutonium fuel element
-  Mixed uranium-plutonium fuel element
-  Al dummy element
-  Rod sample position
-  Source
-  Guide tube

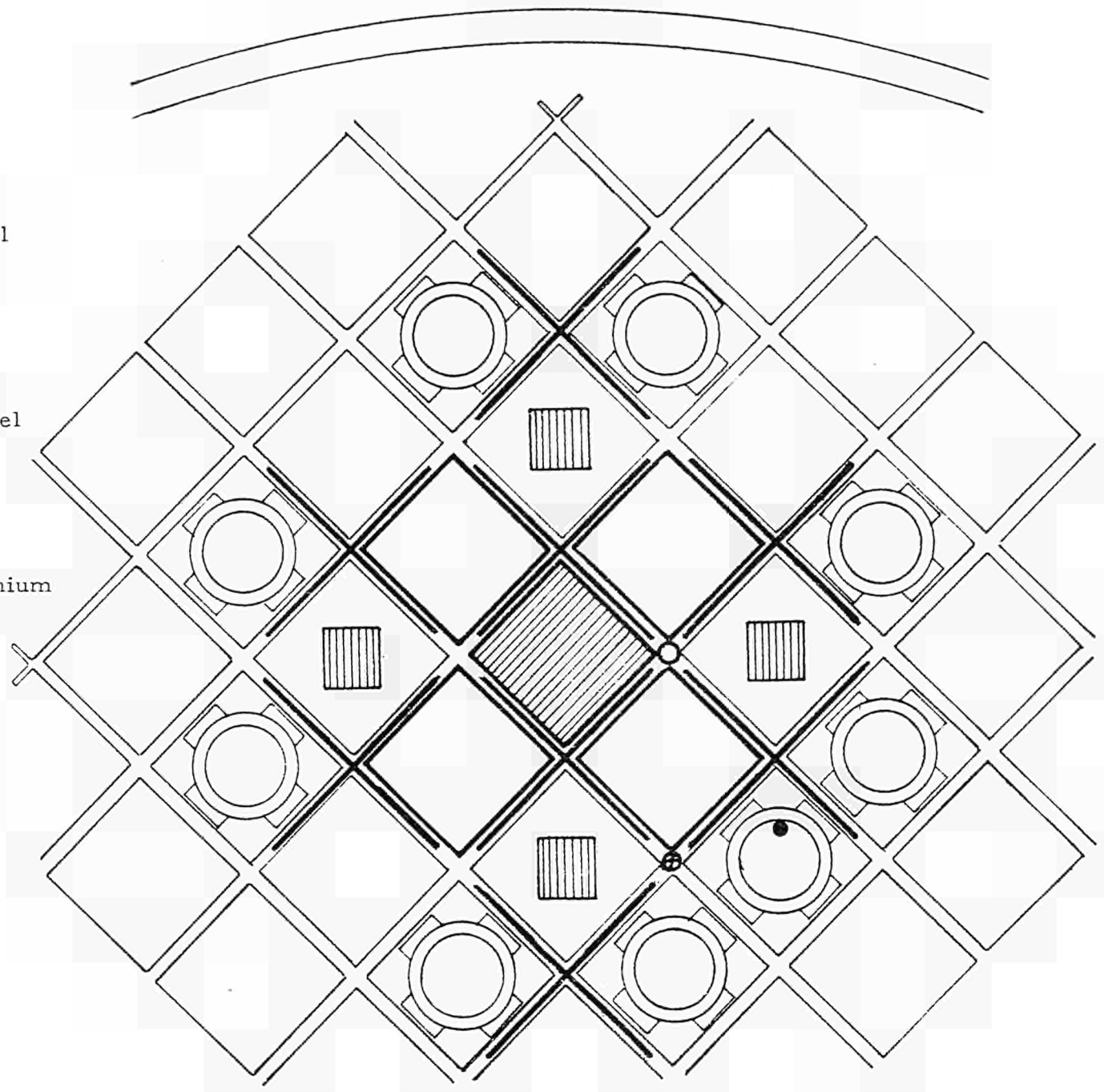


Fig. 6 3x3 fuel element configuration

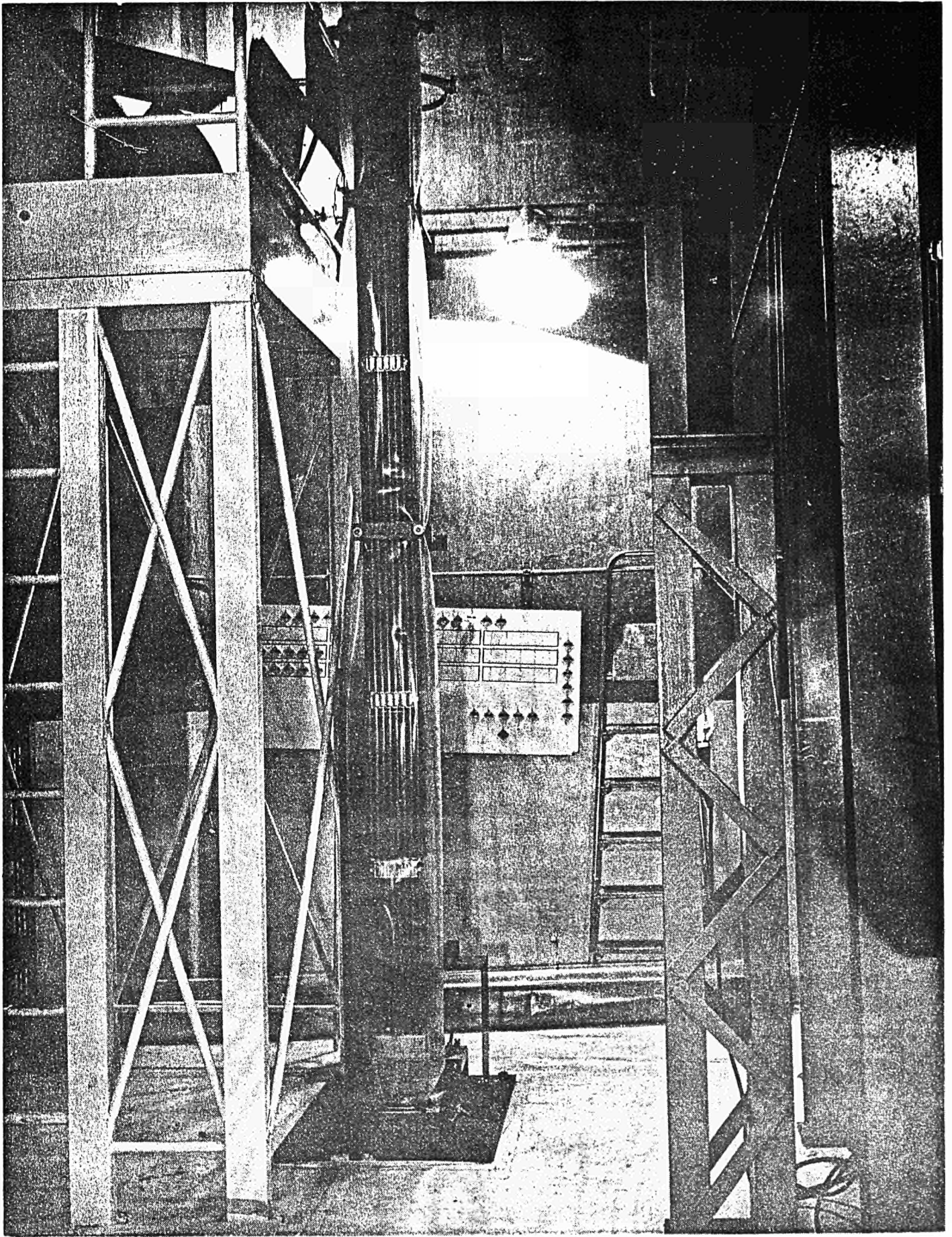


FIG. 7 FUEL VAULT AND STATION EQUIPMENT FOR FUEL ELEMENT INSPECTION AND DISASSEMBLY

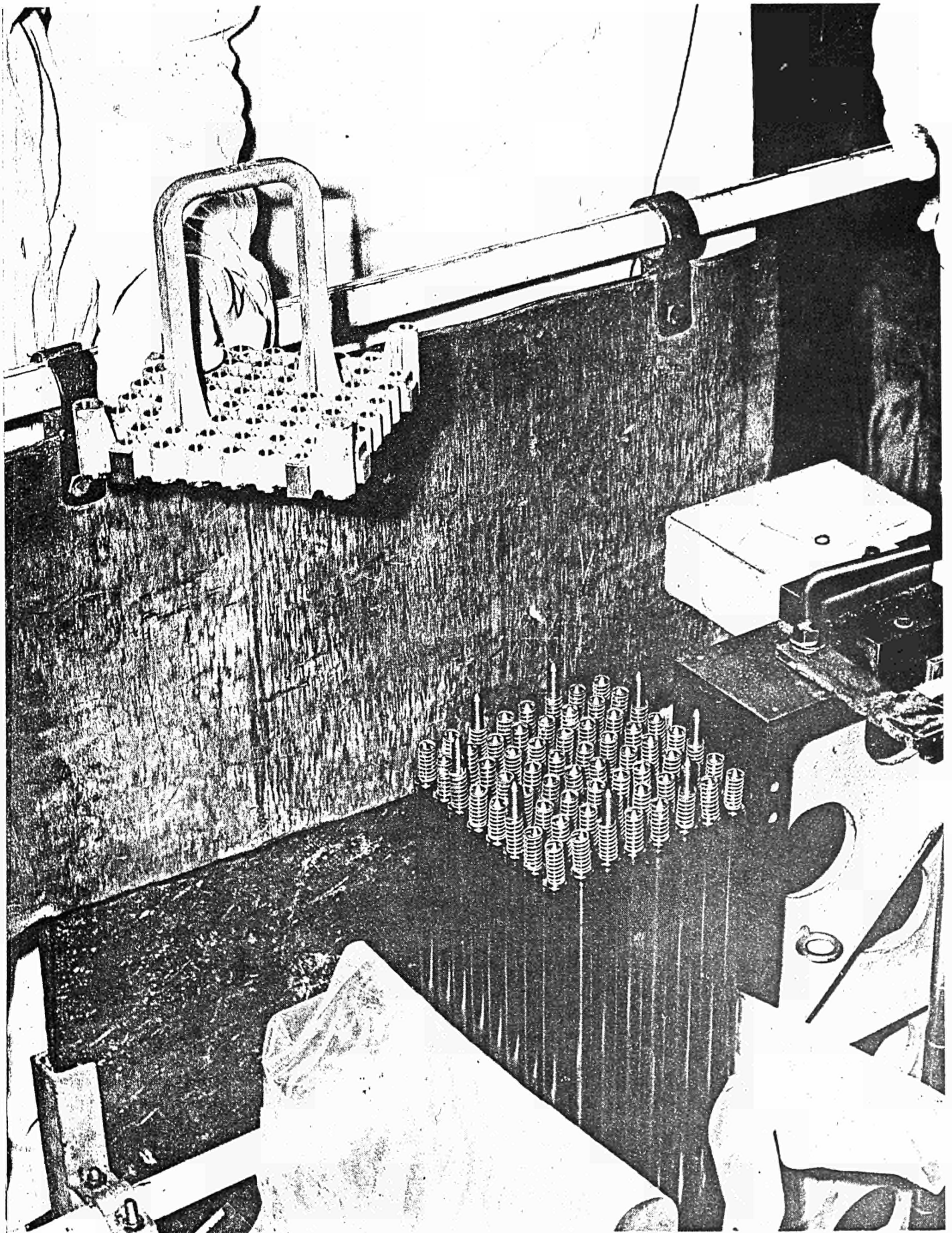


FIG. 8 REMOVAL OF THE UPPER TIE PLATE OF THE FUEL ELEMENT

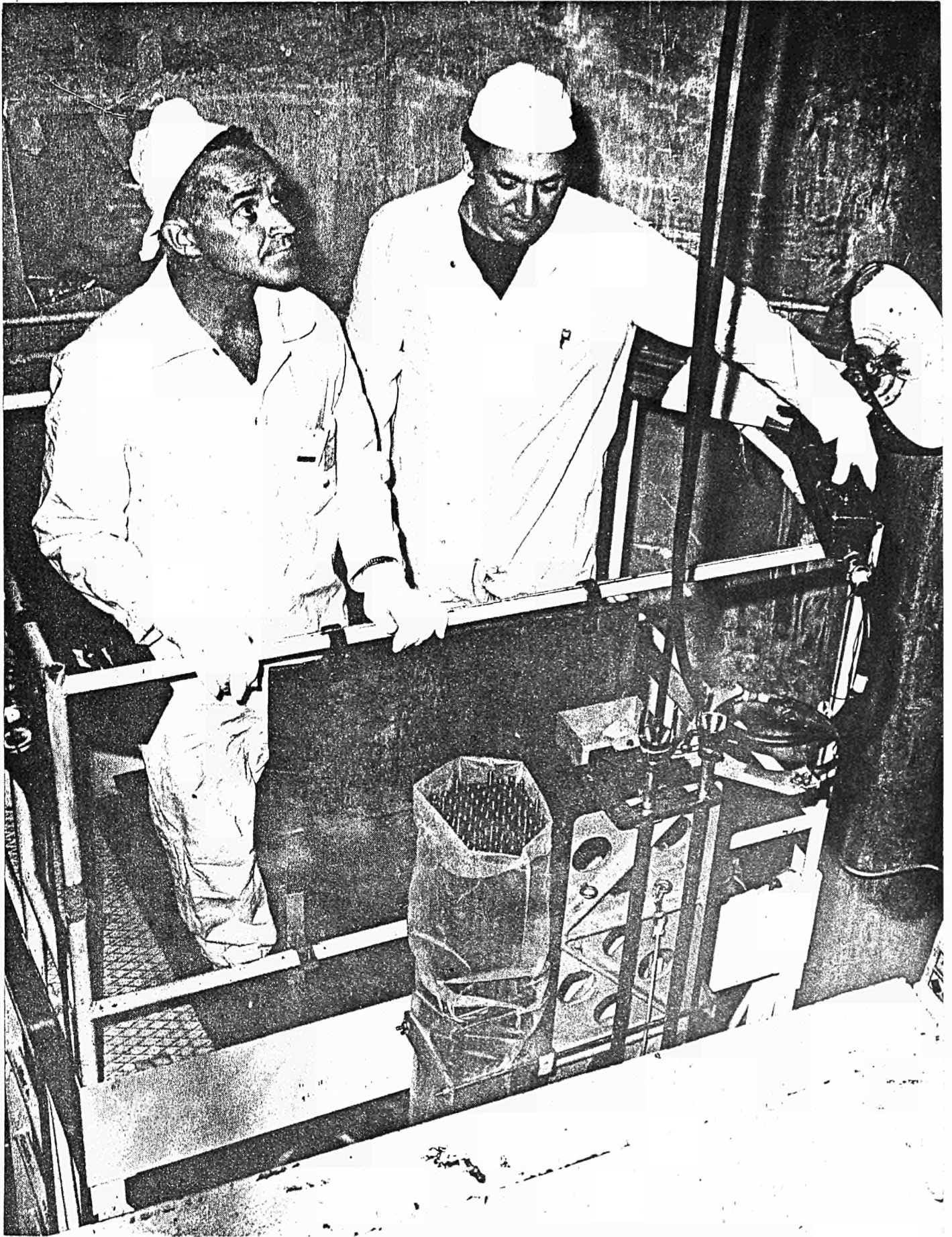


FIG. 9 INSERTION OF THE FUEL ROD IN THE ALUMINUM PROTECTION TUBE

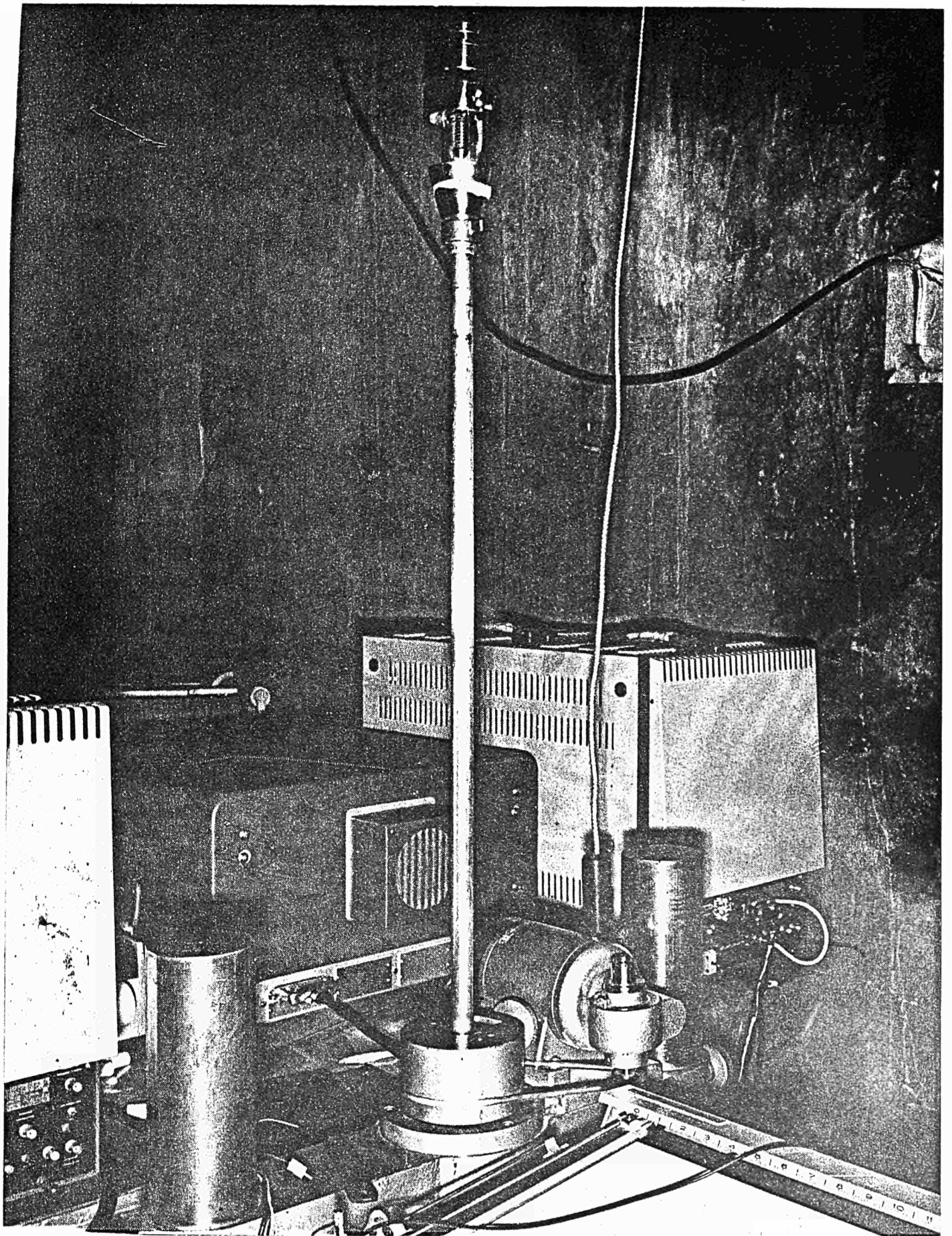


FIG. 10 AUXILIARY SYSTEM FOR ROD POSITIONING AND ROTATION

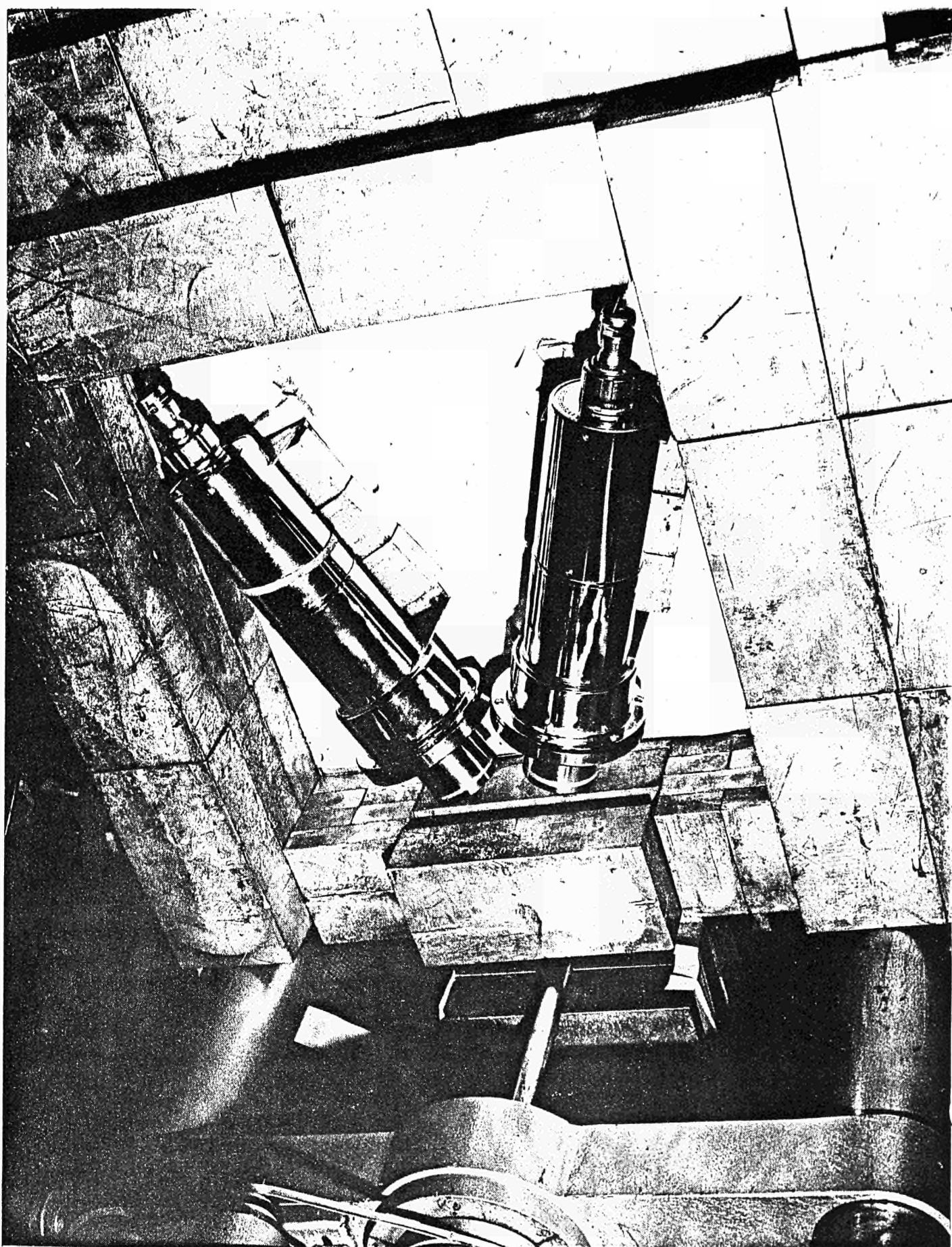


FIG. 11 PHOTOSCINTILLATORS (NaI), SHIELDING AND COLLIMATION SYSTEM

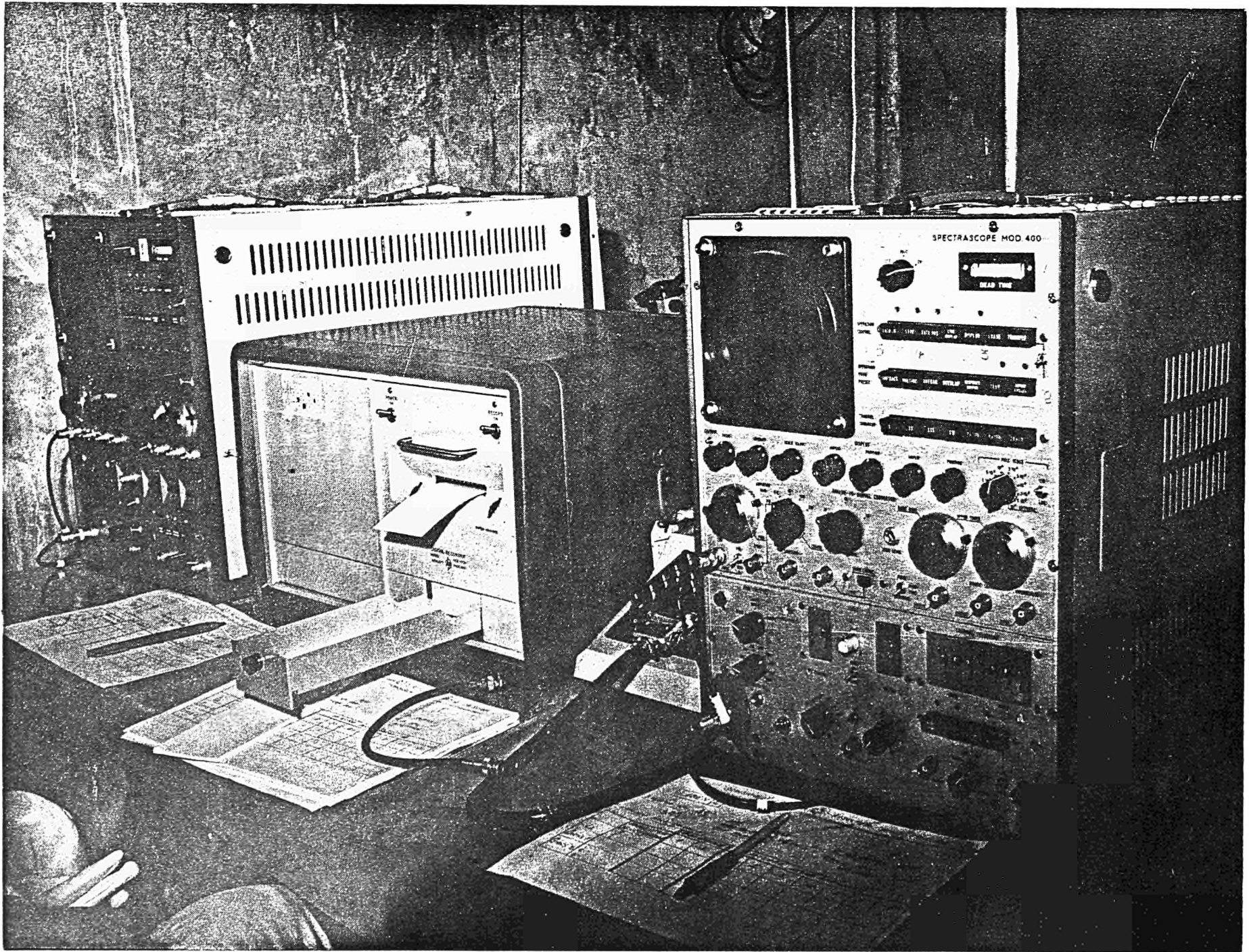
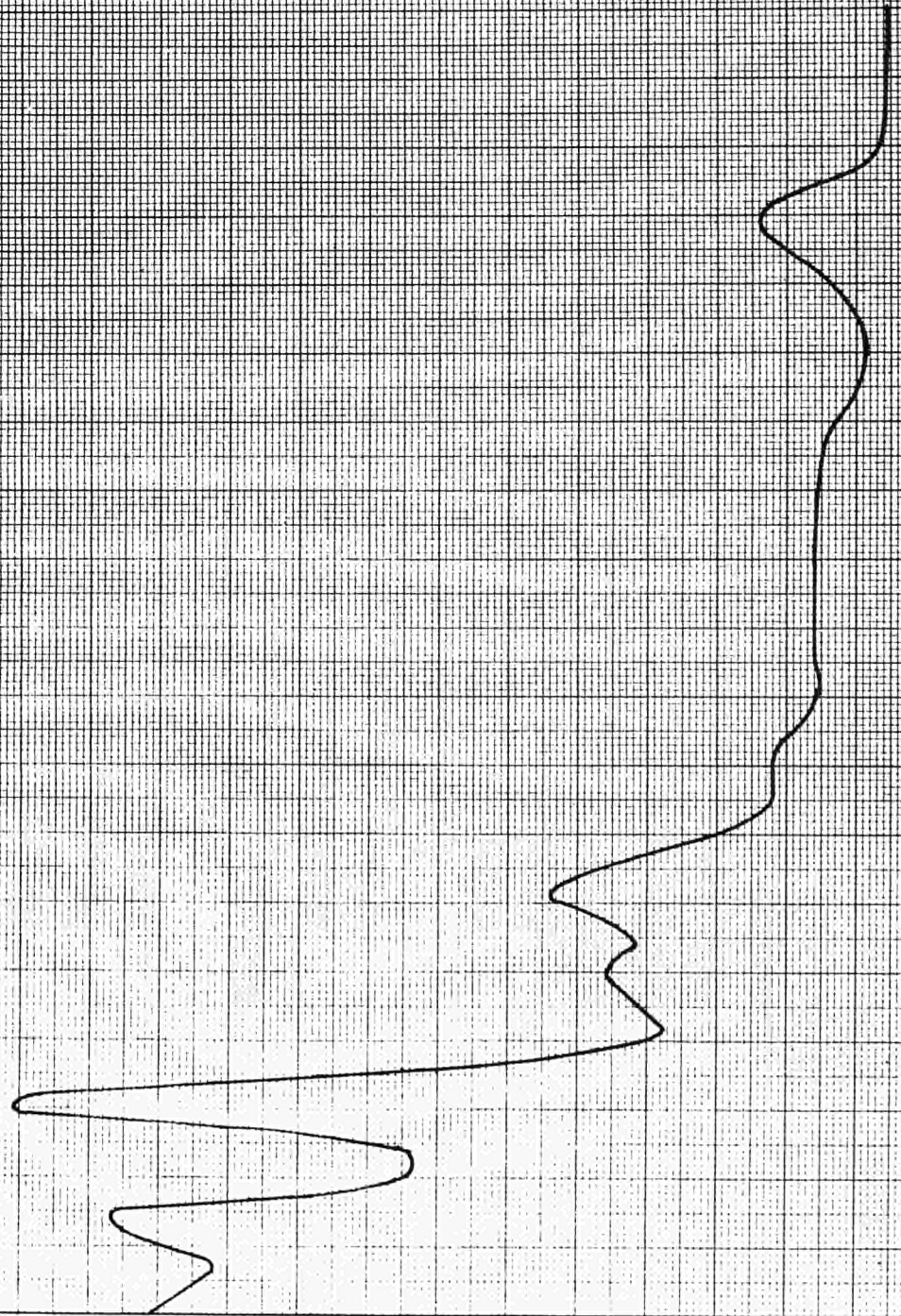


FIG. 12 MULTICHANNEL PULSE ANALYZERS.(400 CHANNELS) AND FAST PRINTER

Fig. 13 SPECTRUM OF ROD GAMMA ACTIVITY OBTAINED BY SCANNING

Counts



0.480 MeV

1.6 MeV

Energy

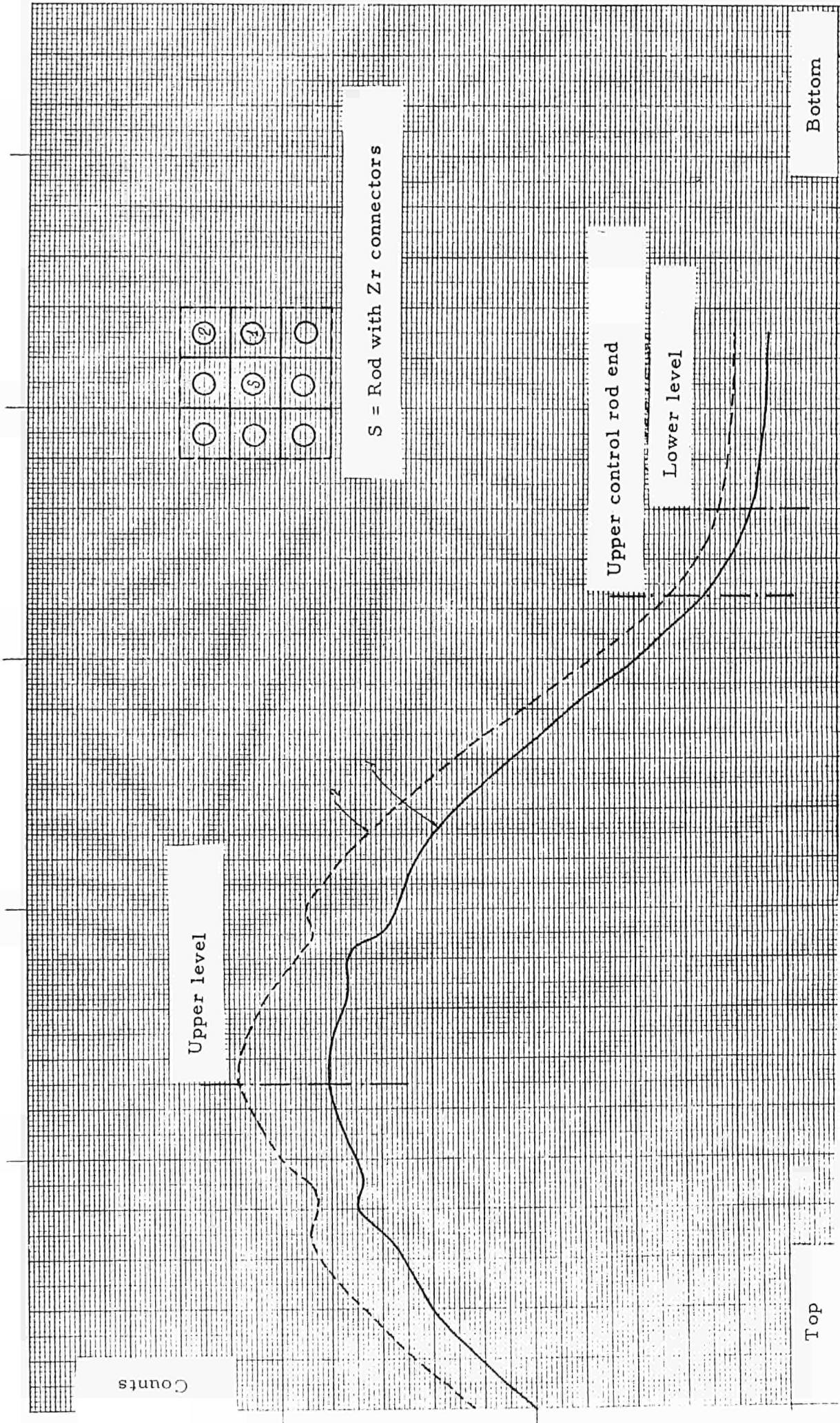


FIG. 14 AXIAL POWER DISTRIBUTIONS IN THE 3x3 FUEL ELEMENT CONFIGURATION

RIFLETTORE

DUMMY

0.468	0.413		0.519	0.573		0.653	0.849
	0.405	0.374	0.517	0.567	0.510	0.660	0.756
		0.467	0.569	0.631	0.642	0.627	
			0.576	0.631	0.777	0.866	1.007
				0.700	0.857	0.958	1.104
					0.883	0.861	
						1.082	1.229
							1.594

0.813	0.704		0.797	0.793		0.702	0.815
0.757	0.760	0.716	0.700	0.704		0.763	0.757
	0.801	0.751	0.740		0.751		
1.071	0.872	0.827	0.814	0.814			1.058
1.147	0.960	0.908	0.886				1.151
	1.063	1.002	0.981	0.987	1.010		
1.217	1.225	1.151	1.115	1.133		1.204	1.215
1.528	1.298		1.460	1.445		1.285	1.529

1.574	1.290		1.514	1.510		1.280	1.565
	1.342	1.156	1.480	1.479	1.139	1.342	
		1.380	1.283	1.287	1.385		
			1.250	1.243	1.288	1.476	1.483
				1.255			1.493
					1.386		
						1.304	
							1.341

DUMMY

RIFLETTORE

S

Fig. 15 Level not affected by the control rods: experimental distribution of the rod power densities.

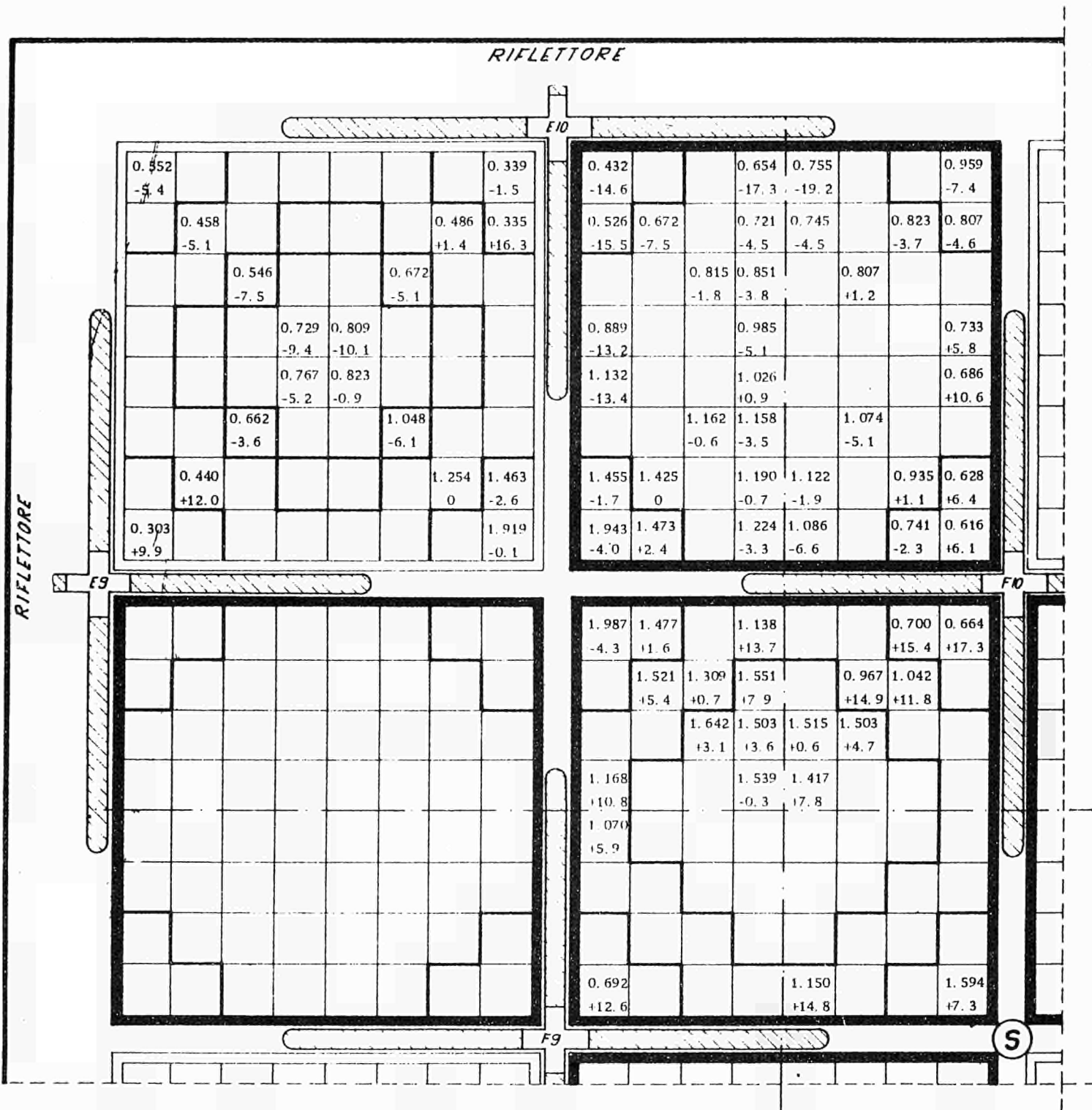


Fig. 16 Level with control rods: experimental distribution of the rod power densities and percentage deviations of theoretical data calculated by RIBOT 5 and SQUID codes. $(\frac{T - E}{E} \cdot 100)$.

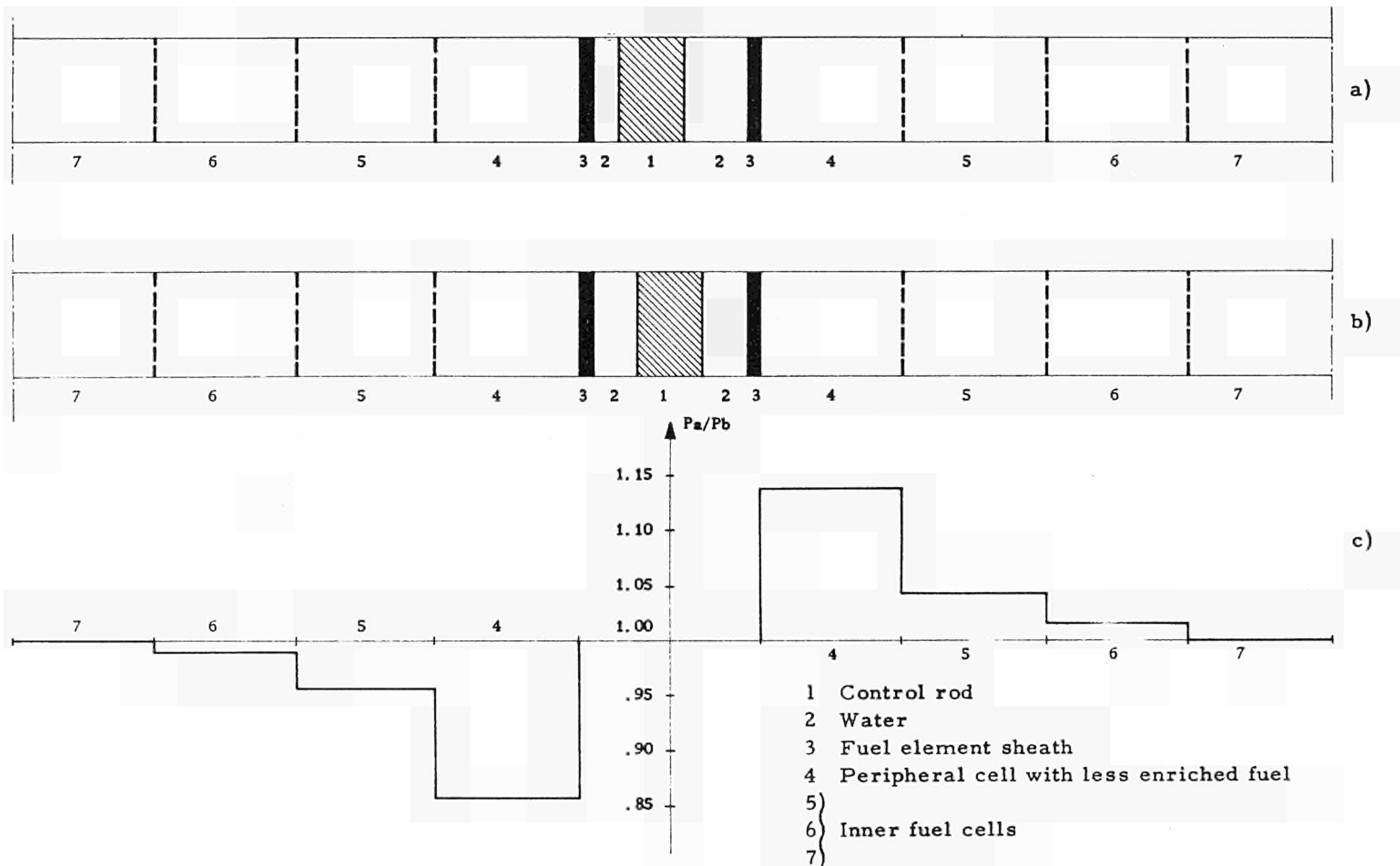


Fig. 17 Evaluation of the effect of off-center control rod positioning:

- a) farthest off-center position
- b) nominal position
- c) ratio between the power densities in the two positions.

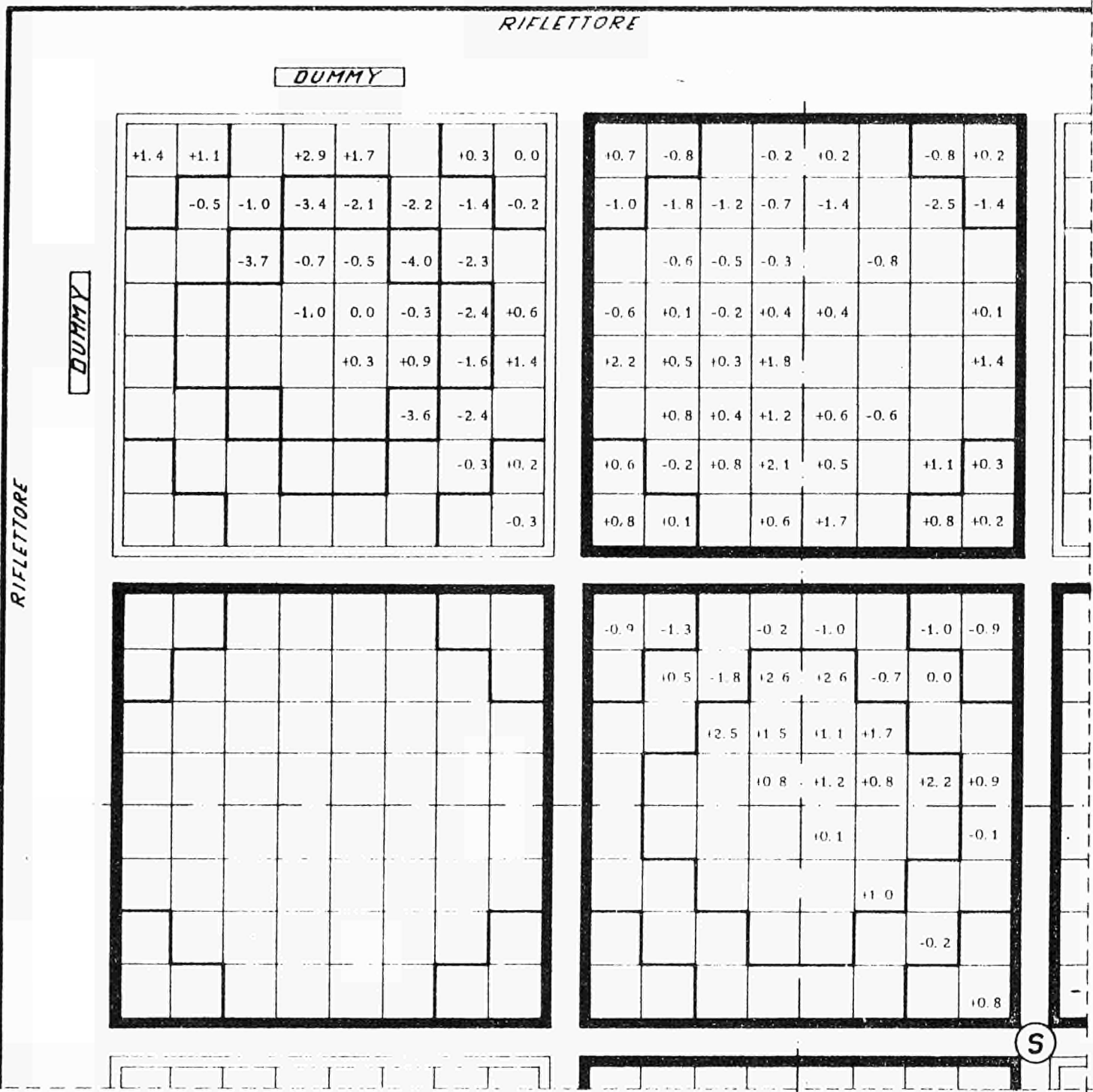


Fig. 18 Level without control rods: percentage deviations between experimental and theoretical rod power densities, as calculated by RIBOT 5 and SQUID codes. $(\frac{T - E}{E} \cdot 100)$. $\sigma = \pm 1.5\%$.

RIFLETTORE

DUMMY

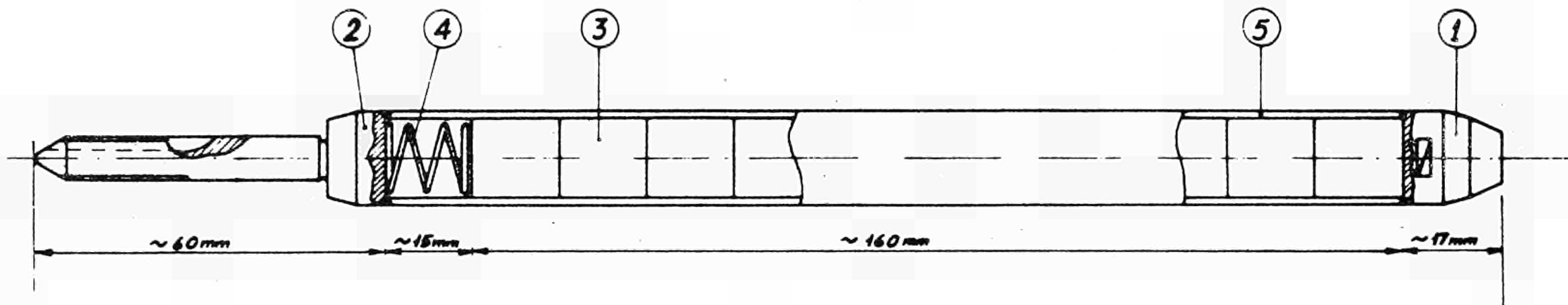
+2.1	+5.4		+6.4	+5.8		+4.1	-0.1
	+4.8	+4.1	+0.1	+2.2	+2.5	+2.0	+0.9
		0.0	+1.1	+1.2	-1.3	0.0	
			-1.8	-0.9	+0.6	0.0	-0.3
				-0.9	+1.6	+0.2	+0.3
					-2.1	-1.5	
						-0.2	-1.3
							-4.0

-0.7	-0.2		+1.2	+1.7		0.0	-0.8
-0.8	+1.4	+0.3	+0.9	+0.3		+1.0	-0.8
	-0.1	+0.4	+0.4		+0.5		
-1.1	+0.1	-0.2	+0.4	+0.4			+0.2
+1.6	+0.1	0.0	+1.2				+1.1
	0.0	0.0	+0.7	+0.1	-0.8		
-1.4	+0.5	-0.2	+1.0	-0.5		+0.5	-1.4
-3.2	-2.2		-1.0	-1.6		-1.2	-3.3

-3.2	-2.9		-2.1	-2.9		-2.1	-2.6
	-0.2	-3.5	+2.0	+2.1	-3.1	-0.1	
		+1.0	-1.2	-1.4	+0.6		
			-3.0	-2.5	-1.5	+2.3	0.0
				-3.3			-0.7
					+0.5		
						+0.2	
							-0.6

S

Fig. 19 Level without control rods: percentage deviations between experimental and theoretical rod power densities, as calculated by FORM, THERMOS and SQUID codes $(\frac{T - E}{E} \cdot 100)$. $\sigma = \pm 1.9\%$.



ITEM	DESCRIPTION	N ^o OFF	MATERIAL
1	END CAP	1	ZIRC. 2
2	THREADED END CAP	1	ZIRC. 2
3	FUEL PELLET	11	P ₂ O ₅ /UO ₂
4	RETAINING SPRING	1	E.N. 49
5	CAN	1	ZIRC. 2

FIG. 20 ENRICHED URANIUM OR URANIUM-PLUTONIUM SAMPLE FOR PRELIMINARY MEASUREMENTS.

Date: 7-5-68

Max. flux peak: $\approx 3 \times 10^9$ n/cm²sec.

Thermal power: 480.8 MW

Electric power: 154 MW

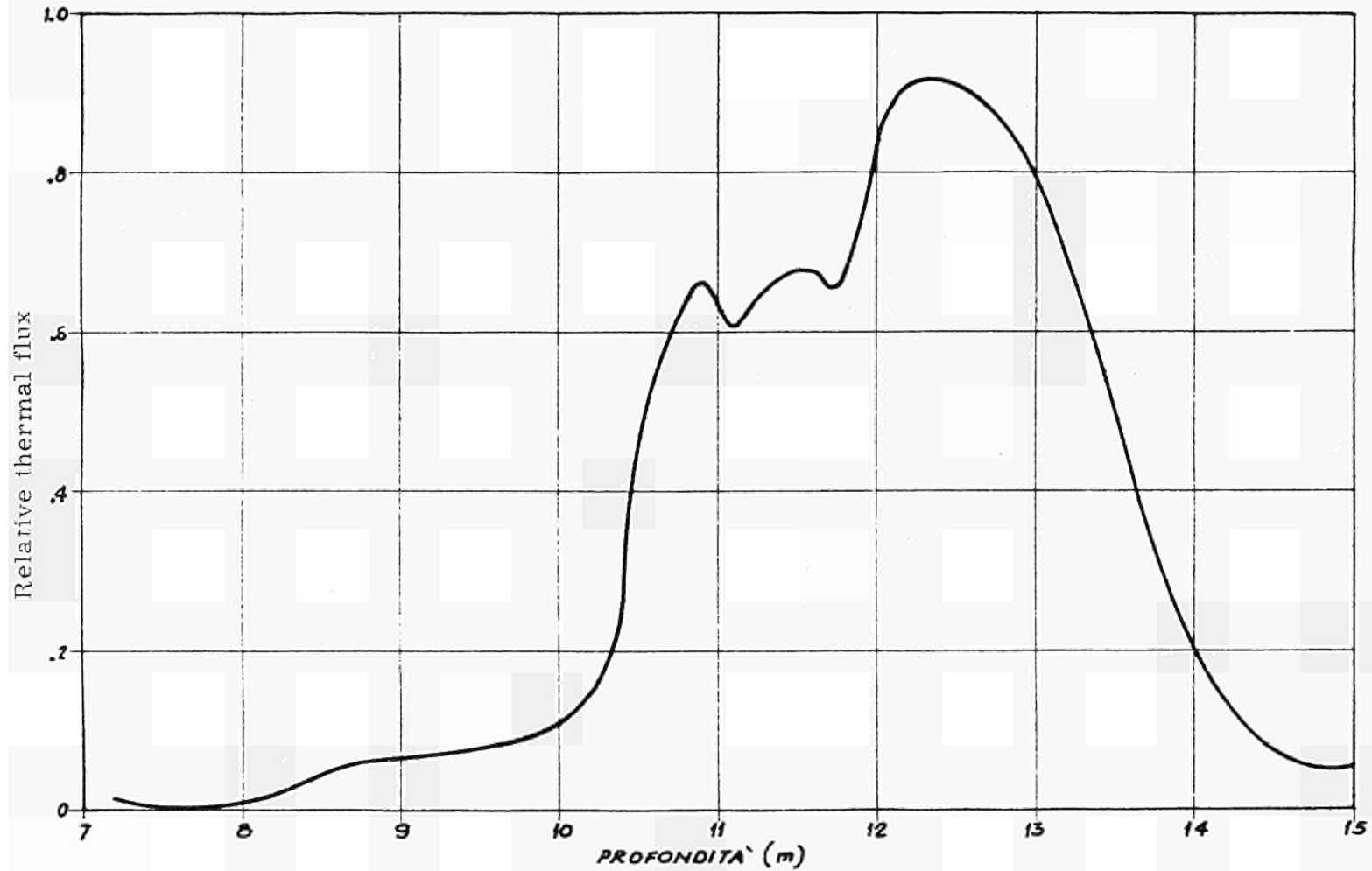


FIG. 21 THERMAL FLUX CURVE ALONG THE CHANNEL SELECTED FOR SAMPLE IRRADIATION.

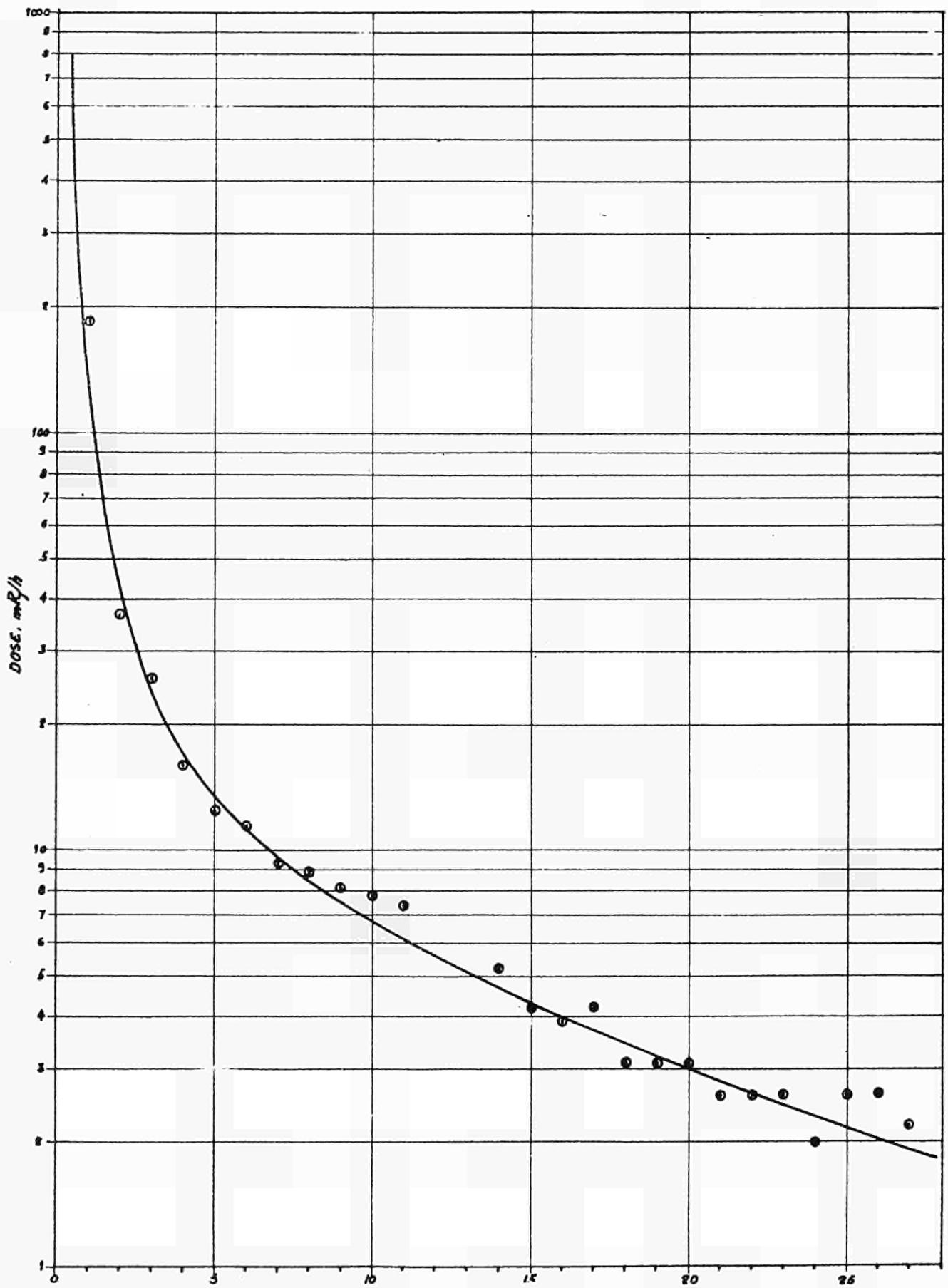


FIG. 22 Dose variation in time for Pu²³⁹C²⁴ (Pu^f 2.855%). The dose corresponds to a flux of 10^9 n/cm² sec.

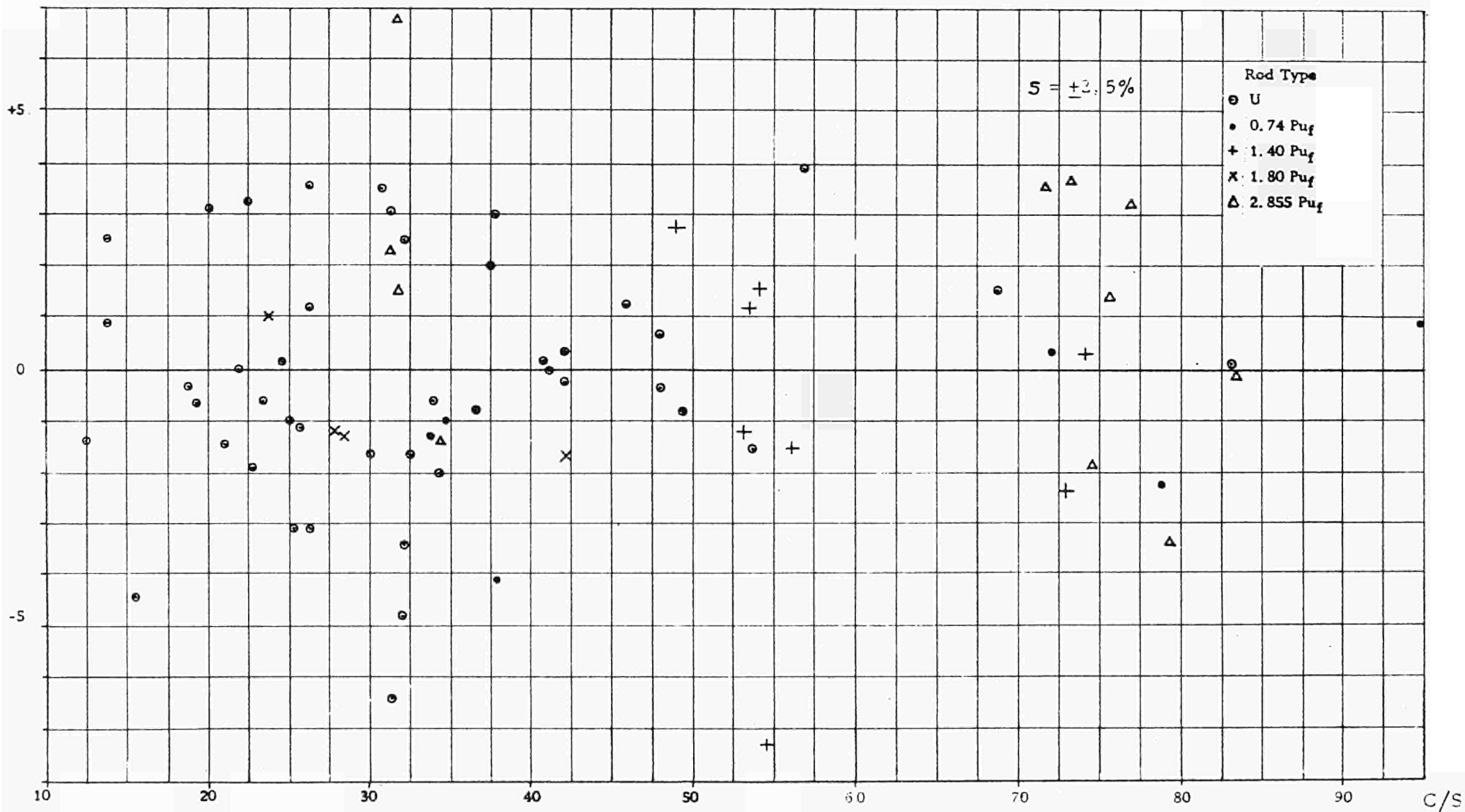
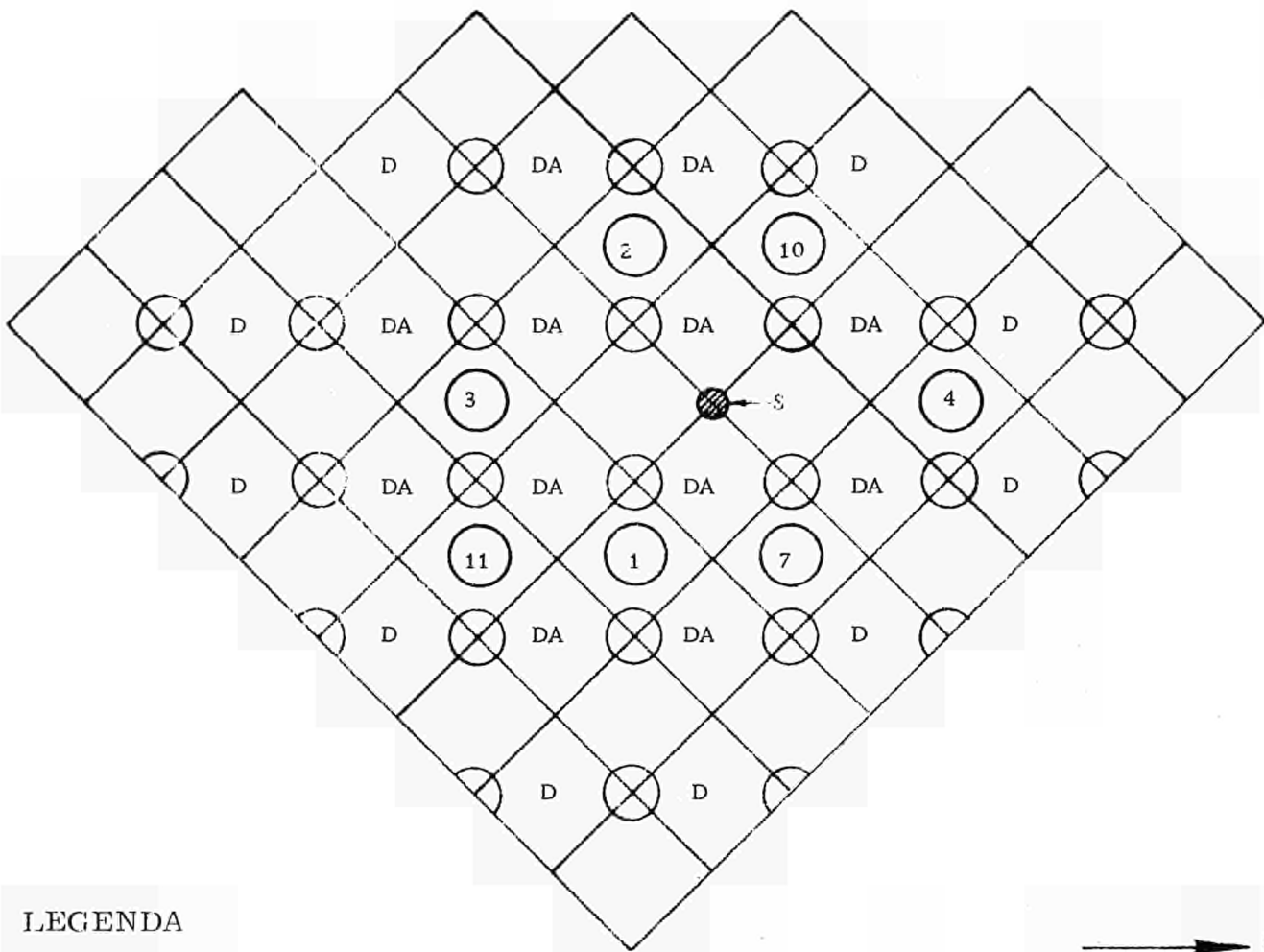
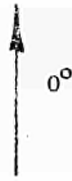


Fig. 23 - Distribution of the percentage differences between the power density values obtained from the total gamma activity data and those obtained from the La-140 gamma activity data



LEGENDA

- D - SS dummy
- DA - Al dummy
- - Instrumentation
- S - Source
- ⊗ - Control rod



FIG. 24 Core configuration before loading enriched uranium minimum critical

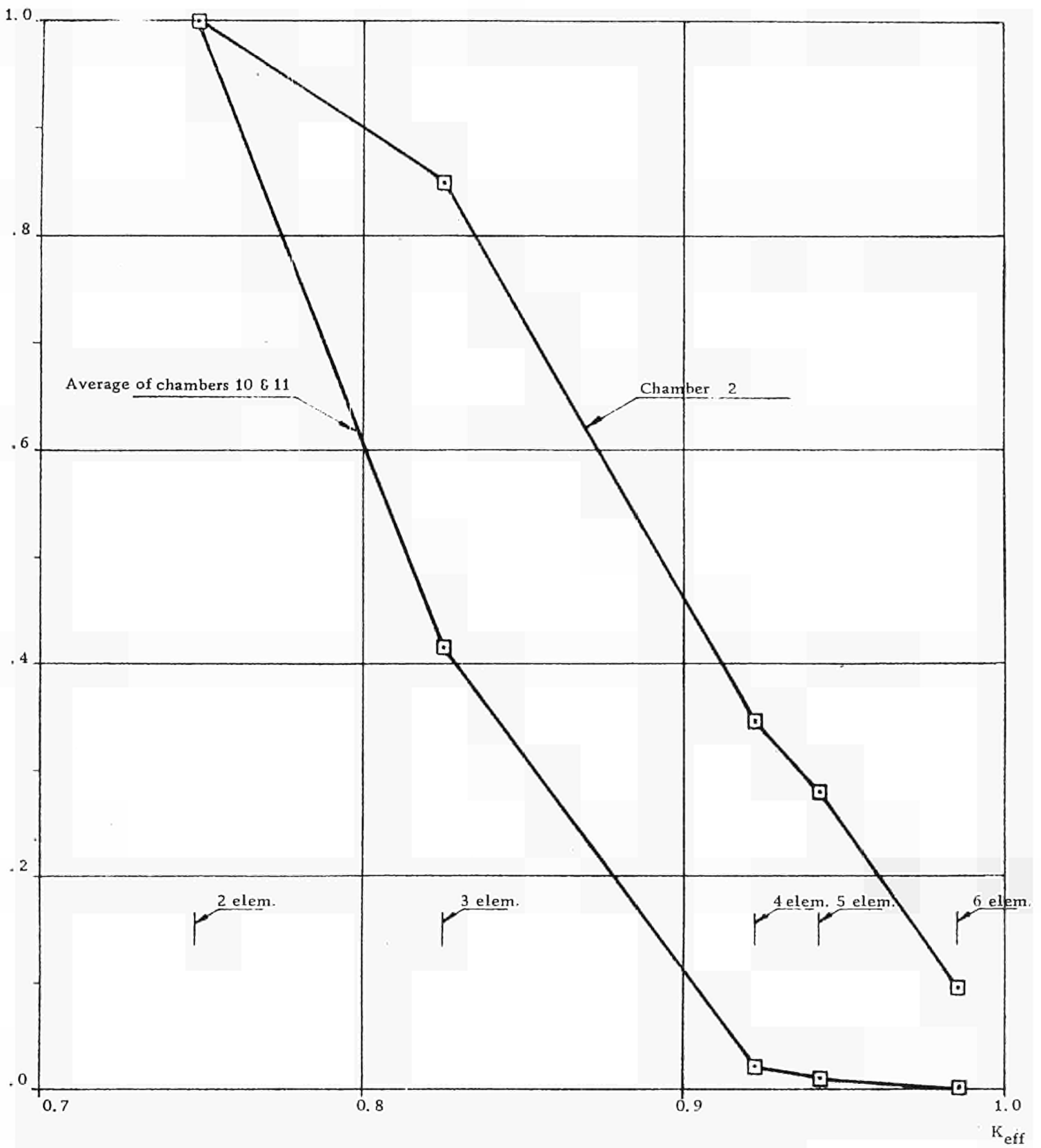


FIG. 25 Inverse count rate enriched uranium minimum critical

ERRATA

CORRIGE

page 9, line 7:	critical assembly	assembly
page 16, line 2	is on	is based on
Appendix I, title	set down of	set down the
page I-5, line 9	Table 4	Table IV
page I-7, lines 10, 16, 25	Table 5	Table V
page I-9, line 1	lanthanum	lanthanum
page I-9, line 6	(20-25 C)	(20-25°C)
page II-1, line 9	heat fluxes	neutron fluxes
page II-1, line 10	n/cm ² /sec	n/cm ² .sec
page II-2, line 1	45 channel	45th channel
page IV-3, lines 2, 3	difference	differences
Fig. 22, title	Pu"C"	Pu-C type
Fig 22, abscissae	--	Days

SECRETARIATO GENERALE ENEL
STAMPA OFFSET - ROMA



EUR 1635. f

Le prix de ce rapport ayant été omis,

veuillez noter qu'il est de

225, - FB.

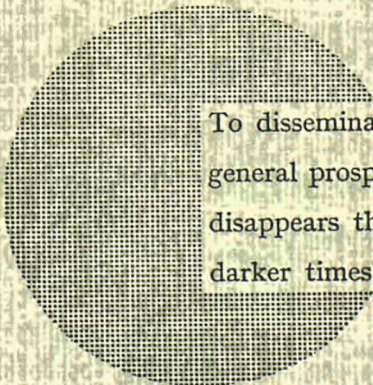
NOTICE TO THE READER

All Euratom reports are announced, as and when they are issued, in the monthly periodical "euro abstracts", edited by the Center for Information and Documentation (CID). For subscription (1 year : US \$ 16.40, £ 6.17) or free specimen copies please write to :

Handelsblatt GmbH
"euro abstracts"
Postfach 1102
D-4 Düsseldorf (Germany)

or

**Office de vente des publications officielles
des Communautés européennes**
37, rue Glesener
Luxembourg



To disseminate knowledge is to disseminate prosperity — I mean general prosperity and not individual riches — and with prosperity disappears the greater part of the evil which is our heritage from darker times.

Alfred Nobel

SALES OFFICES

All reports published by the Commission of the European Communities are on sale at the offices listed below, at the prices given on the back of the front cover. When ordering, specify clearly the EUR number and the title of the report which are shown on the front cover.

SALES OFFICE FOR OFFICIAL PUBLICATIONS OF THE EUROPEAN COMMUNITIES

37, rue Glesener, Luxembourg (Compte chèque postal N° 191-90)

BELGIQUE — BELGIË

MONITEUR BELGE
Rue de Louvain, 40-42 - 1000 Bruxelles
BELGISCH STAATSBLAD
Leuvenseweg 40-42 - 1000 Brussel

LUXEMBOURG

OFFICE DE VENTE DES
PUBLICATIONS OFFICIELLES DES
COMMUNAUTÉS EUROPÉENNES
37, rue Glesener - Luxembourg

DEUTSCHLAND

BUNDESANZEIGER
Postfach - 5000 Köln 1

NEDERLAND

STAATSDRUKKERIJ
Christoffel Plantijnstraat - Den Haag

FRANCE

SERVICE DE VENTE EN FRANCE
DES PUBLICATIONS DES
COMMUNAUTÉS EUROPÉENNES
26, rue Desaix - 75 Paris 15^e

ITALIA

LIBRERIA DELLO STATO
Piazza G. Verdi, 10 - 00198 Roma

UNITED KINGDOM

H. M. STATIONERY OFFICE
P. O. Box 569 - London S.E.1

Commission of the
European Communities
D.G. XIII - C.I.D.
29, rue Aldringer
Luxembourg

CDNA04475ENC